Frequency and Voltage-dependent Electrical Parameters, Interface Traps, and Series Resistance Profile of Au/(NiS:PVP)/n-Si Structures

Murat Ulusoy (ulusoymurat@gazi.edu.tr)
Gazi Üniversitesi: Gazi Universitesi https://orcid.org/0000-0001-9842-0318
Ş. Altındal
Gazi Üniversitesi: Gazi Universitesi
Perihan Durmuş
Gazi Üniversitesi: Gazi Universitesi
Süleyman Özçelik
Gazi Üniversitesi: Gazi Universitesi
Yashar Azizian Kalandaragh
Gazi Üniversitesi: Gazi Universitesi

Research Article

Keywords: Organic (NiS:PVP) interfacial film, C-V-f and G/ω-V-f -V characteristics, Frequency-voltage dependence, Admittance Method

Posted Date: March 18th, 2021

DOI: https://doi.org/10.21203/rs.3.rs-309986/v1

Frequency and voltage-dependent electrical parameters, interface traps, and series resistance profile of Au/(NiS:PVP)/n-Si structures

M. Ulusoy[1,*], Ş. Altındal[1], P. Durmuş[1], S. Özçelik[2,3], Y. Azizian Kalandaragh[2,3,*]

[1]Department of Physics, Faculty of Sciences, Gazi University, Ankara, Turkey
[2]Photonics Application and Research Center, Gazi University, 06500 Ankara-Turkey
[3]Photonics Department, Applied Science Faculty, Gazi University, 06500 Ankara-Turkey

Abstract

A thin (NiS-doped PVP) interface layer was spin-coated on n-Si substrate and between Au contact were prepared on the surface by the sputtering method and then their basic electrical features for example diffusion-potential (V_D), doping density of donor-atoms (N_D), Fermi-energy (E_F), barrier-height (Φ_B), and depletion layer-width (W_D) were extracted reverse-bias C^{-2}-V plots as function frequency and voltage. The voltage profile of interface/surface-states (N_{ss})/ relaxation-times (τ), and series resistance (R_s) were also obtained from the admittance and Nicollian-Brews method, respectively. Strongly frequency-dependent and voltage especially in both accumulation and depletion regions due to the existence of N_{ss}, R_s, and polarization as well as (NiS-doped PVP) organic interlayer. At low frequency, the observed higher value of C and G shows that thin (NiS:PVP) interlayer can be successfully used to obtain high charges/energy storage (MPS) structure/capacitor instead of conventional insulator layer performed traditional methods. As a result, the observed important changes in electrical parameters with frequency and voltage depend on N_{ss}, their τ, R_s, organic interlayer, and interfacial or dipole polarization.

Keywords: Organic (NiS:PVP) interfacial film; C-V-f and G/ω-V-f -V characteristics; Frequency-voltage dependence; Admittance Method

[*]Corresponding author: ulusoymurat@gazi.edu.tr, yasharazizian@gazi.edu.tr

1. Introduction

In electronics and semiconductor physics, the value of C and G of the electronic devices such as a diode, photovoltaic devices, and capacitor increase with increasing voltage, and hence C-V and G-V plots show three different zones, and they are called inversion, depletion, and accumulation regions. The practical status is maybe different in these regions because of the existence of these N_{ss}, interlayer, R_s, and polarization. Therefore, the quality of electronic devices by an organic interface layer is dependent on different parameters like the interface/surface states (N_{ss}), surface-morphology/preparation, the thickness and permittivity of the interlayer, series-resistance (R_s), the doping level of acceptor/donor-atoms (N_a/N_d) and their uniformity, frequency, voltage, and temperature [1-9]. When an oxide interlayer for example semiconductor insulator, metal, organic material, and ferroelectric performed between metal and semiconductor interface, MS structure turns into MIS, MPS, and MFS type structure and then gains capacitor features which can store electronic charges or energy [10-13]. Many N_{ss} or dislocations may be occurred in the fabrication process of the electronic devices due to energy localization in the bandgap of the semiconductor and interface layer.

The relationship between the surface-state charging process and C/(G/w) of these structures under an external circuit was well interpreted by Nicollian & Goetzberger [5]. R_s value is effective on the performance of these structures and the voltage and frequency dependence of it can be extracted from impedance/admittance technique investigated by Nicollian & Brews [4] method by using the measured capacitance/conductance (C_m/G_m) data. But the real value of R_s of these structures is corresponding to the obtained experimental results of C and G at accumulation-zone (C_{ma}/G_{ma}) at adequate high frequency ($f \geq 0.5$MHz). The effects of R_s may be eliminated by making C/G-V measurements at low or intermediate frequencies, which means that both the N_{ss} and R_s have a significant effect on the electrophysical properties of the fabricated device which should be considering the calculation to get more precise results [14-17]. While N_{ss} is more important both in depletion and inversion zone at low-moderate frequencies, R_s is effective only at accumulation zone at high frequency. The charges at traps/states can easily follow the alternating ac signal and hence may be produced an excess capacitance/conductance (C_{ex}/G_{ex}) to the real value of them by depending on their life/relaxation-time (τ) of them and the frequency or period of the measured C and G values [4,7-13].

Polyvinyl- pyrrolidone/alcohol (PVP, PVA) is semi-crystalline and it has a wide range of crystallinity and some advantages are high water/alcohol-solubility and easy formation of hydrogen bonding, and special dielectric properties [17,18]. For this respect, both PVP and

PVA are more important and so they can be used as an organic interlayer in the construction of metal-polymer-semiconductor (MPS) electronic devise [9,11,14,15,19-25]. Although polymers have low mobility and permittivity, they can be increased by doped with some materials such as Ni, Co, graphene, Zn, ZnO, CdS, Fe_3O_4 [14-21,26,27].

The first aim of this study is to use (NiS-doped PVP) organic interlayer instead of conventional insulators and then investigate their basic electrophysical features for example diffusion-potential (V_D), doping density of donor atoms (N_D), Fermi energy (E_F), barrier height (Φ_B), and depletion layer width (W_D) as function voltage and frequency. The next purpose is to the extracted voltage-dependent profile of N_{ss}, their relaxation-times (τ), and R_s. For these two aims,

Both voltage-frequency dependences of C and G/ω were performed in wide range frequency (1 kHz-1MHz) and voltage (-2V/+3V). The measured electrophysical parameters show strong frequency dependence features in the depletion and accumulation region. The reason of these effects are because of the existence of N_{ss}, R_s, and polarization as well as (NiS-doped PVP) organic interface layer.

2. Experimental Details

In the first step, for preparation of NiS nanostructures, 0.2 M from Nickel chloride.6H2O (NiCl2 , KBR) was dissolved in 40ml distilled water and stirred 30min, then 0.5M Na2S.3H2O(LOBA Chemie) added to solution drop by drop until pH of solution be 7. Then by adding the 0.5M NaOH(Merk), reserved pH=14. 15min by Power =180 in Microwave device, then the precipitate was washed five times in water and kepts to dry in Oven for 48 hours. Finally, the precipitate was annealed in 1000 centigrade. at the end of process green powder was obtained.

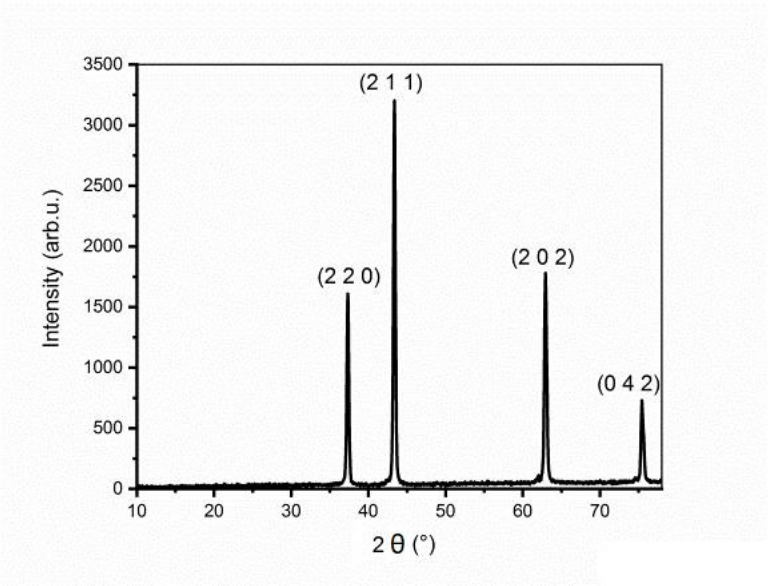

Fig 1. XRD pattern of NiS nanostructures prepared by microwave- assisted method

XRD pattern of preparation NiS has been shown in Fig 1. Peak least is according to JCPDS file No. 86 – 2281, and this is expresses preparation the NiS without any impurities.

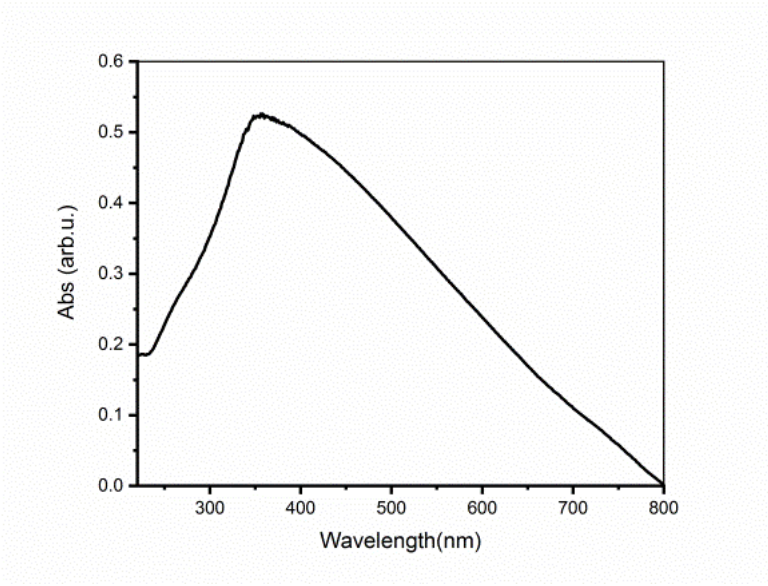

Fig 2. Absorbance spectrum of NiS nanostructures prepared by microwave- assisted method

Absorbance spectrum of NiS has been shown in Fig 2. Absorbance peak of NiS calcined in 1000 ºC, is in 380nm.

The MPS type SBDs were prepared on an n-type (phosphorus-doped) Si wafer with 300 µm thick and 4 Ω cm resistivity. Firstly, it was cleaned in H2O, H_2O_2, and NH_4OH (3:1:1) solution at 70 °C in the ultrasonic bath and then rinsed in the high-resistivity deionized water at a prolonged time. Secondly, ohmic contact with Au (99.999%) with 150 nm thick was prepared by thermal evaporation method on the other side of the Si wafer at the pressure of 10^{-6} Torr.

The prepared film was annealed at 500 ºC in the nitrogen-atmosphere for 5 minutes. After the formation of Ohmic-contact. Firstly, prepared NiS nanostructures in powder form were dissolved in deionized water as used solvent to obtain PVP solution (8% w/w), while was heating up to 80°C temperature and mixture for 3h. NiS-PVP solutions were mixed at room condition and then coated onto the front of the n-Si wafer by a spin coating method (SCM) because of its higher spin-velocity and longer spin-times leads to create a thinner film on the semiconductor substrate. Therefore, the prepared (NiS-PVP) solution was grown on the front side of the n-Si wafer by the SCM. Finally, Au rectifier contacts with 7.85×10^{-3} cm ^{2} areas and 150 nm thick were formed on the (NiS-PVP) interlayer at 10^{-6} Torr. Both back-ohmic and front-rectifier contacts were performed by using the BESTEC thermal evaporation system which four crucibles has made by tungsten to evaporate different metals onto substrate/semiconductor and metal-thickness-meter. Both the schematic diagram of the formed Au/(NiS:PVP)/n-Si structures and the measured impedance or admittance measurement system were given in Fig. 1 (a) and (b), respectively. HP 4192A LF impedance analyzer and a I-V measurement system were used for C-V and G/ω-V analyses.

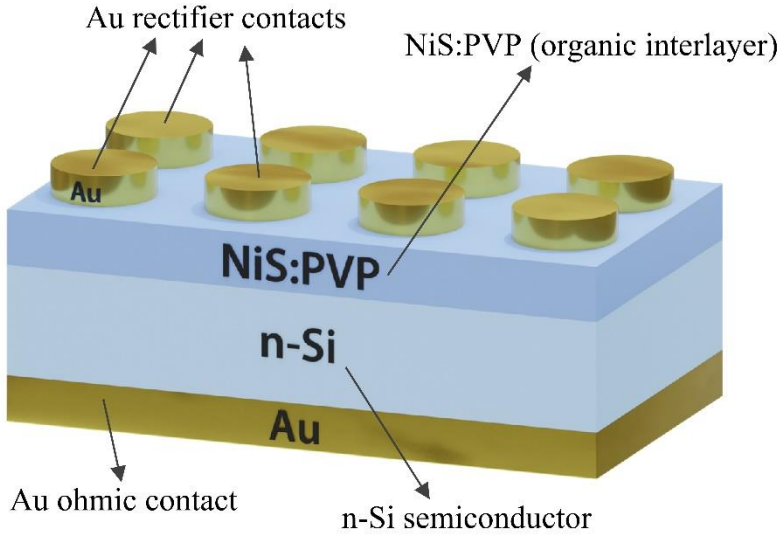

(a)

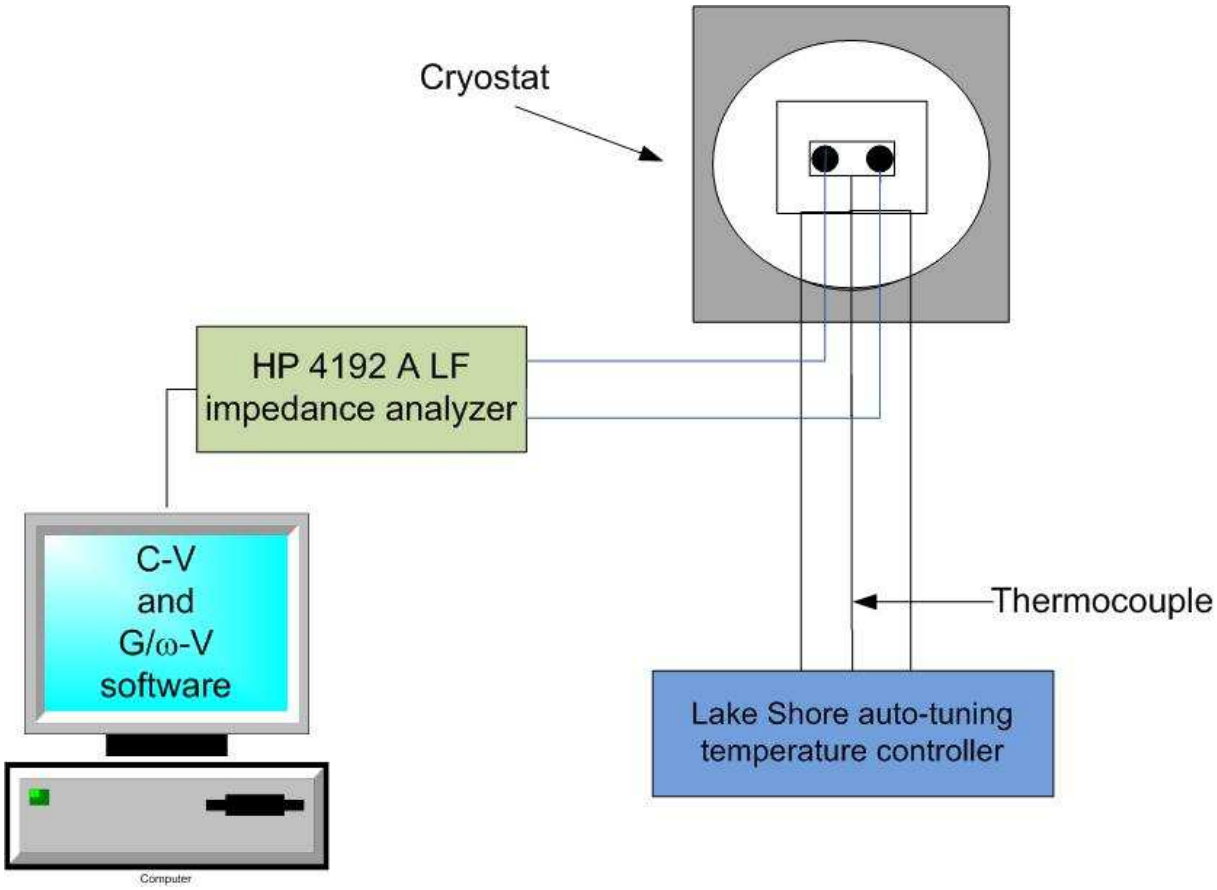

(b)

Fig. 3: **a)** A schematic diagram of the Au/(NiS:PVP)/n-Si structures and **b)** the setup of the measured admittance/impedance measured system

3. Experimental Results

C-V and G/ω-V characteristics of the fabricated Au/(NiS:PVP)/n-Si Schottky structure are presented in Fig 2. in frequencies from 1kHz to 1MHz and voltages -2V to 3V. As indicated in these two figures, both the C-V and G/ω-V plots have three zones depends on the accumulation ($V \geq 1.6V$), depletion ($0 \leq V \leq 1.6V$), and inversion ($-2V \leq V \leq 0V$) regions for intermediate and high frequencies like a MOS type capacitor.

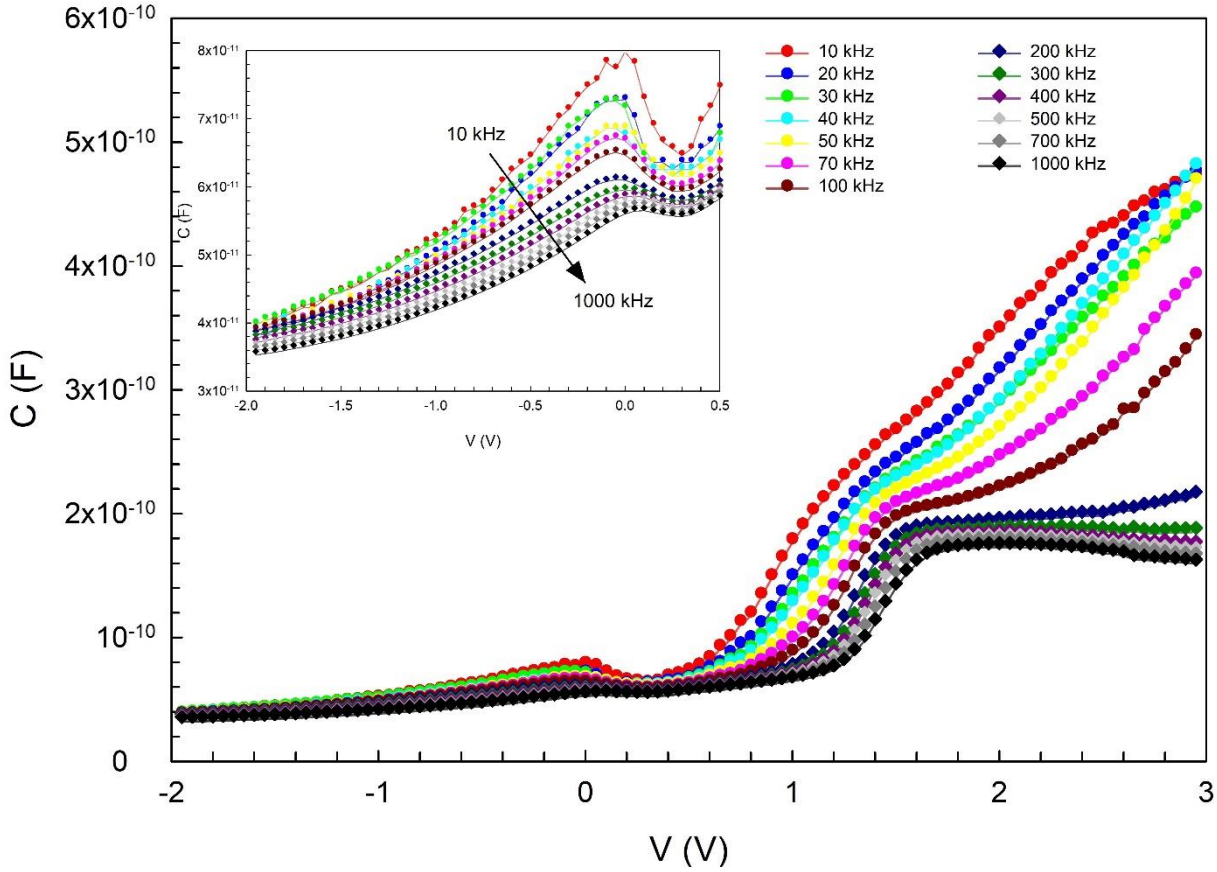

Fig. 4. The plot of C-V characteristics of the Au/(NiS:PVP)/n-Si structure for various frequency.

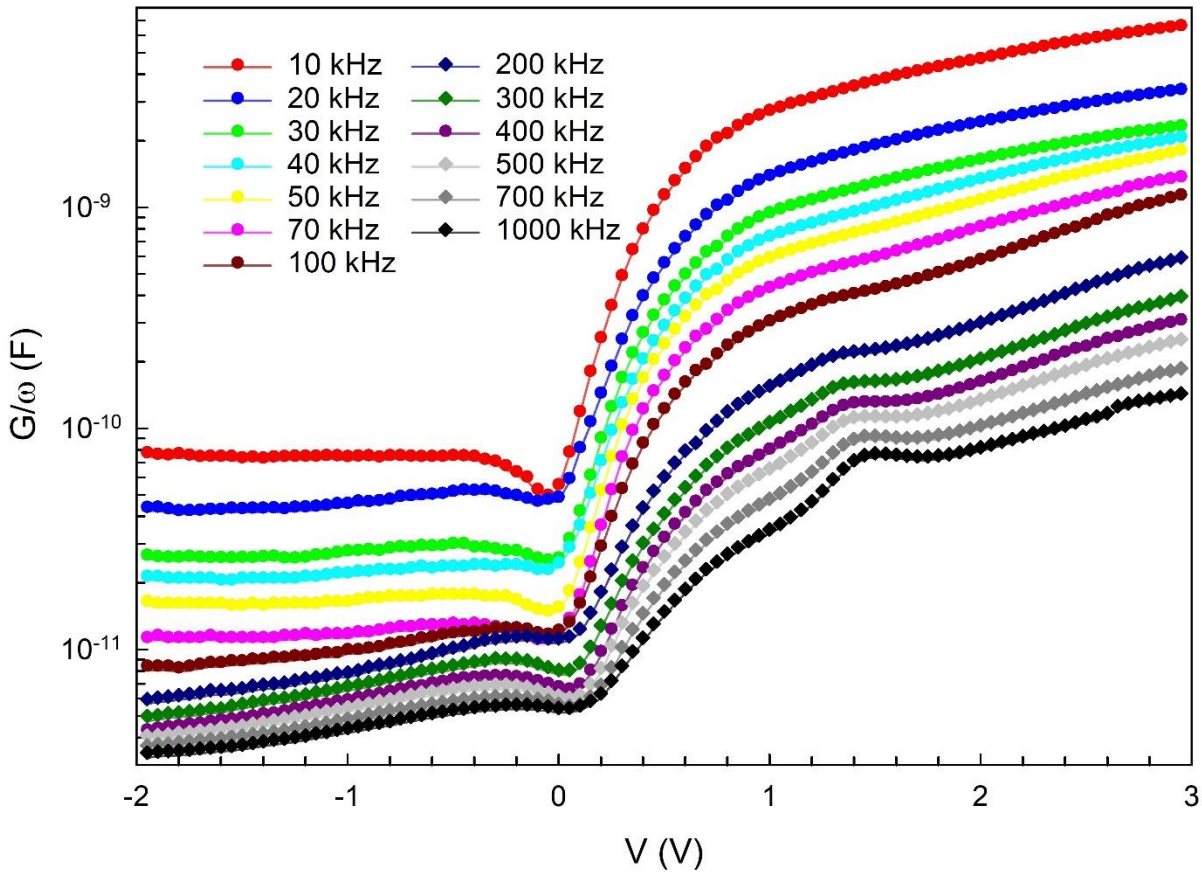

Fig. 5. The plot of G/ω-V characteristics of the Au/(NiS:PVP)/n-Si structure for various frequency.

It is seen inset in Fig. 2, C-V plots at zero-voltage or in the weak inversion region because of a special distribution of N_{ss} and dipole or surface polarization for low and intermediate frequencies [1,4-10]. Because there are many kinds of N_{ss} and they have different relaxation/life-times (τ) and at low frequencies are depend on alternating ac signal. Because at very low or intermediate frequencies, the electronic charges located at any traps or surface-states can be easily followed an alternating ac signal and hence supplied both an excess C and G to the real value of them contrary to high frequencies because of the relaxation-time (τ) of them have not enough time to charge movement by ac current. [4-10].

On the other hand, for low-frequencies, the polarization mechanism in the interfacial layer can change the trap mechanisms. In general, there are different polarization process and all of them depends on the ac electric field and frequency, which are electronic, atomic, dipole, and interfacial/surface polarization [28]. But, among them, while electronic and atomic polarization are effective only at very high frequencies (10^{10}-10^{15} Hz), but dipole and interfacial polarizations are effective only at low frequencies or a few kHz, respectively. Therefore, in the measured frequency range of 10 kHz-1 MHz in this study the last two types of polarization

which are usually known Maxwell-Wagner type polarization. While the R_s and interlayer are effective only at accumulation or high forward bias voltages at high frequencies, N_{ss} is an effective bot in depletion and weak inversion regions at low frequencies. If the MS structure has R_s, N_{ss}, and an interfacial layer, applied bias voltage (V_a) across the structure will be shared among them as ($V_a=V_i+V_{Rs}+V_D+V_{ss}$).

As can be seen in Fig.2, the C-V plot shows a concave curvature at the accumulation region especially due to the existence of R_s and interlayer. Therefore, both the draw of the N_{ss} and R_s versus frequency for various bias voltage in depletion region by using the C-V and G/ω-V data are more important. The high-value of R_s may be created errors in electrical parameters especially at the accumulation region, but this effect may be minimized utilizing the proper washing and cleaning process of the semiconductor surface and device preparation processes, and applying a correction or/adjustment these measurements before the desired information is extracted. The voltage-dependent profile of the resistance (R_i) can be extracted from the Nicollian and Brews in the whole measured frequency and voltage range diode. But, according to this method, the value of R_i at high-frequencies ($f \geq 0.5$ MHz) is corresponding to the real value of R_s for MOS or MPS type structures and capacitors and can be calculated from the measured capacitance and conductance at a strong accumulation-zone (C_{ma} and G_{ma}) data as following [24]:

$$R_s = \frac{G_m}{G_m^2 + \left(\omega C_m\right)^2} \tag{1}$$

To determine the effects of the R_s on the impedance/admittance based on measured C-V and G/ω-V, the voltage-dependent profile of R_i was calculated by using Eq. (1) for each frequency and is illustrated in Fig. 4. The value of conductance (G=1/R) is related to R_s. In other words, the decrease of R_s at the accumulation region for high frequencies is the result of the increase of conductance. As can be seen in Fig. 4, the R_i-V plots have a peak and while the magnitude of peak decreases with increasing frequency, peak position shifts towards to accumulation region due to reordering and restructuring of surface states under the electric field.

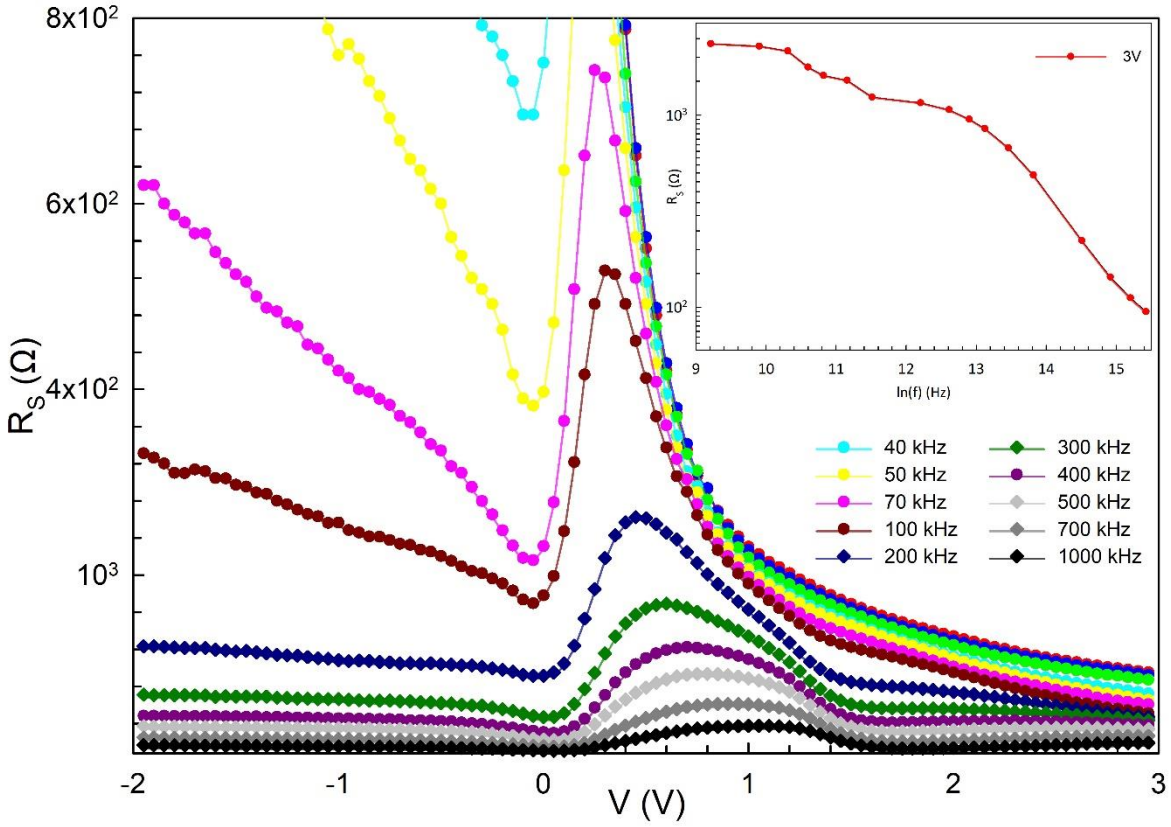

Fig. 6. The plot of R_i-V and Rs-ln(f) characteristics of the Au/(NiS:PVP)/n-Si structure for various frequencies.

Therefore, the measured C_m-V and G_m/ ω-V curves of the MPS structure for adequate high frequency (2 MHz) were corrected as C_c-V and G_c/ω-V curves and given in Fig 5 (a) and (b), by using the following relations, respectively.

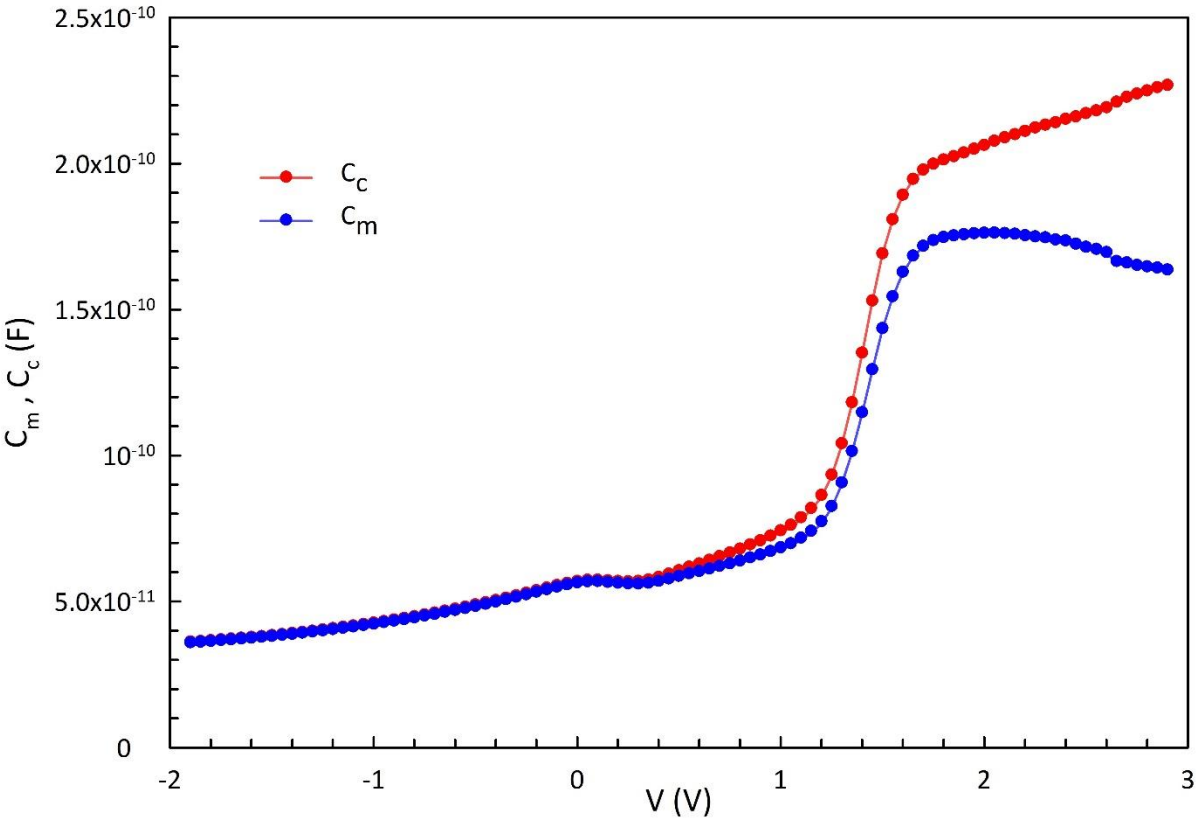
2.5x10-10
2.0x10-10
1.5x10-10
10-10
5.0x10-11
0
Cm , Cc (F)
Cc
Cm
-2
-1
0
1
2
3
V (V)

(a)

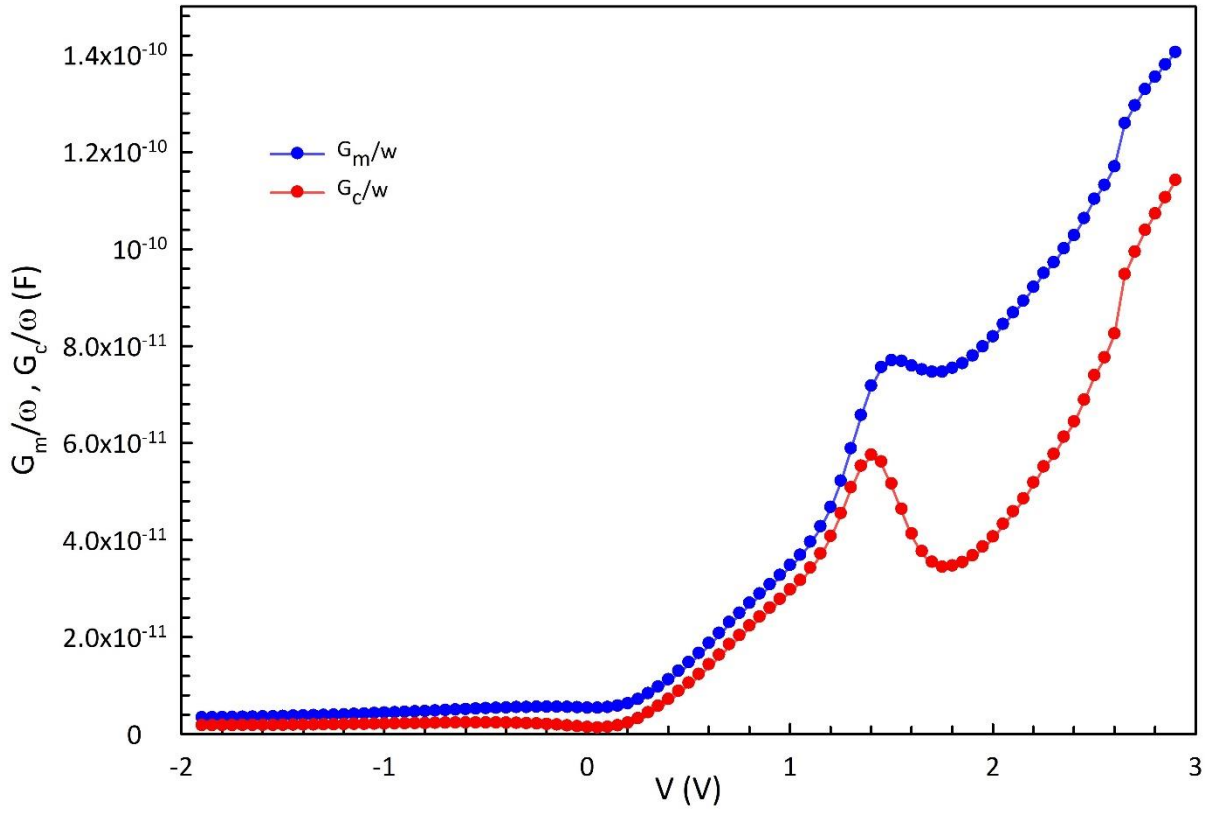
1.4x10-10
1.2x10-10
10-10
8.0x10-11
6.0x10-11
4.0x10-11
2.0x10-11
0
Gm/ω , Gc/ω (F)
Gm/w
Gc/w
-2
-1
0
1
2
3
V (V)

(b)

Fig. 7. (a) The plots of C_m-V and C_c-V characteristics of the Au/(NiS:PVP)/n-Si structure for 1 MHz. and **(b)** The plots of G_m/ω-V and G_c/ω-V characteristics of the Au/(NiS:PVP)/n-Si structure for 1 MHz.

As shown in these figures, the corrected value of C_c increases with increasing voltage and the observed concave-curvature of C_m-V curve at the accumulation region becomes disappears due to the elimination R_s effect. But, the corrected G_c/ω-V curve becomes decreases and give a peak at about 1.45 V. As can be clearly seen in Fig. 5 (a) and (b), the value of R_s is more effective on the C_m-V and G_m/ω-V curves for high frequencies and hence should be taken into account in the calculation in the admittance measurements.

$$C_c = \frac{\left[G_m^2 + (\omega C_m)^2\right] C_m}{a^2 + (\omega C_m)^2} \quad \text{and} \quad G_c = \frac{[G_m^2 + (\omega C_m)^2)]a}{a^2 + (\omega C_m)^2} \tag{2}$$

$$\text{Here, } a = G_m - [(G_m)^2 + (\omega C_m)^2]R_s.$$

The electrophysical parameters of the prepared Au/(NiS:PVP)/n-Si structure such as $V_D=V_o+kT/q$, N_D, E_F, W_D, E_m, and N_{ss} were extracted from the linear part of the reverse-bias$1/C^2$-V plots for each frequency by [1,2].

$$C^{-2} = \frac{2(V_R + V_o)}{q\varepsilon_s\varepsilon_o A^2 N_D} \tag{3}$$

$$N_D = \frac{2}{q\varepsilon_s\varepsilon_o A^2 \tan\theta} = \frac{2\left(\frac{dV}{dC^{-2}}\right)}{q\varepsilon_s\varepsilon_o A^2} \tag{4}$$

$$E_F = \frac{kT}{q}\ln\left(\frac{N_C}{N_D}\right) \tag{5}$$

$$E_m = \left(\frac{2qN_D V_o}{\varepsilon_s \varepsilon_o}\right)^{0.5} \tag{6}$$

In Eqs. (3-6); A is the area of rectifier-contact, ε_s is the dielectric-constant of semiconductor (ε_s =11.8 ε_o for Si), ε_o is the dielectric-constant of vacuum, N_C is the density of states at conduction- band (E_c). The reverse bias C^{-2}-V characteristics of the Au/(NiS:PVP)/n-Si structure measured at room temperature for various frequency is given in Fig.6. As can be seen in Fig. 6, these plots have a good linear relation in the wide voltage range of -1.6V-(-0.5 V). While the value of intercept-voltage ($V_o=V_i$) was extracted from the intercept of the C^{-2}-V

plot f at zero-bias voltage, N_D was extracted from the slope of this plot for each frequency. As can be also seen in Fig. 6, the used an enough thick interfacial layer leads to a large intercept voltage which is becoming higher than the bandgap of a semiconductor depends on surface states. Therefore, the value of V_o was modified by using the constant (c_2) which is given as following [2]:

$$c_2 = \frac{\varepsilon_i}{\varepsilon_i + q^2 \delta N_{ss}} \cong \frac{N_D(\exp.)}{N_D(theor)} \tag{7}$$

Since the value of c_2 is closer to 1 then the value of N_{ss} is closer to zero, c_2 is closer to zero then the value of N_{ss} becomes very high. Therefore, both the mean value of N_{ss} for each frequency was calculated by using Eq. 6 and was tabulated in Table 1. Thus, the modified value of BH was calculated by using the following relation for each frequency:

$$\Phi_B(C-V) = \left(c_2 V_0 + \frac{kT}{q} \right) + E_F = V_D + E_F \tag{8}$$

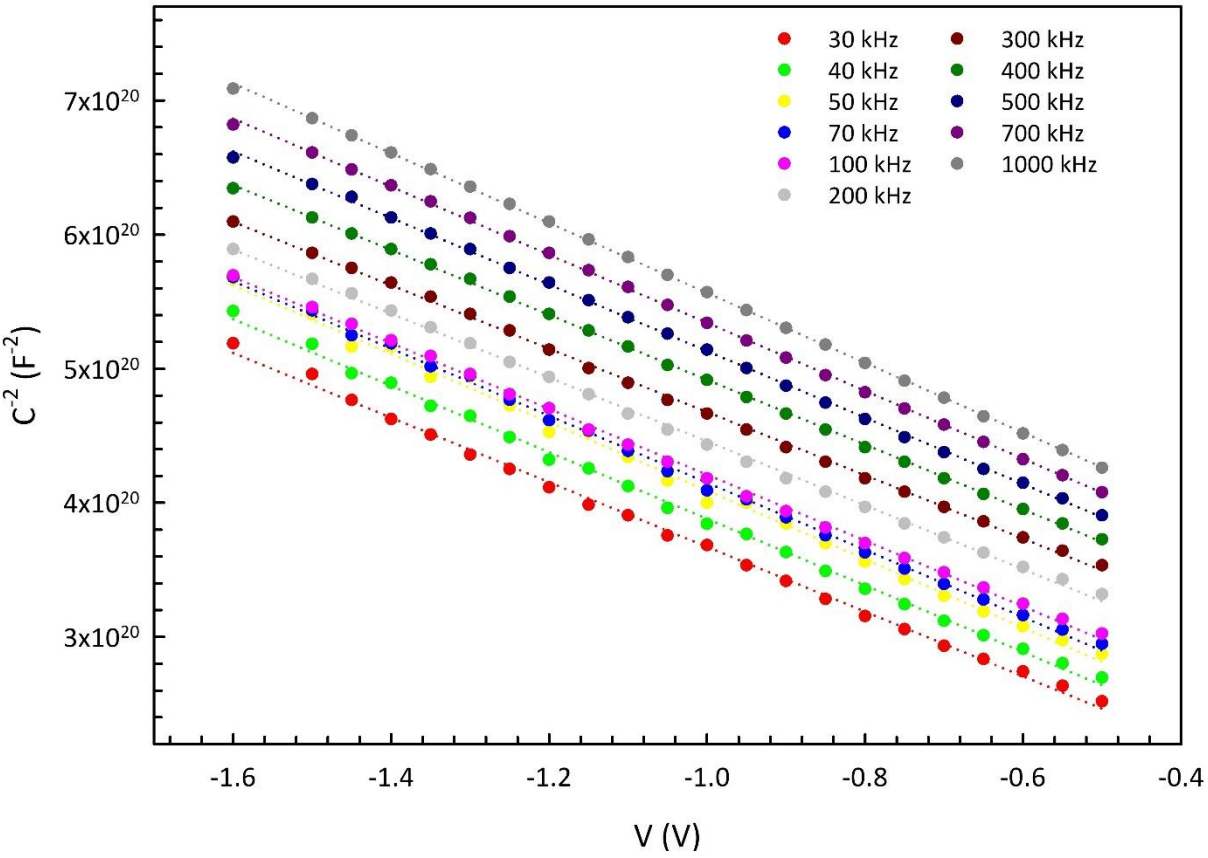

Fig. 8. The plot of C^{-2}-V characteristics of the Au/(NiS:PVP)/n-Si structure was measured for various frequencies.

Table 1. The values of various basic parameters for Au/(NiS:PVP)/n-Si structure calculated

from the C-V and G/ω-V plots in the frequency range of 10-1000 kHz.

f (kHz)	V_D (eV)	N_D 10^{14}x(cm^{-3})	E_F (eV)	c_2	Φ_B (eV)	W_d (μm)	E_m (kV/cm)	N_{ss}(from Eq.7) 10^{11}x ($eV^{-1}cm^{-2}$)
10	0.295	6.79	0.266	0.566	0.443	72.0	1.98	8.49
20	0.415	7.10	0.265	0.591	0.520	84.7	2.83	7.65
30	0.477	7.24	0.264	0.603	0.562	90.3	3.27	7.28
40	0.552	7.41	0.263	0.618	0.614	96.3	3.79	6.84
50	0.610	7.54	0.263	0.628	0.656	101.0	4.21	6.54
70	0.655	7.65	0.263	0.637	0.689	104.0	4.53	6.30
100	0.746	7.86	0.262	0.655	0.759	109.0	5.18	5.83
200	0.899	8.16	0.261	0.680	0.880	118.0	6.27	5.20
300	0.995	8.53	0.261	0.696	0.960	123.0	6.95	4.84
400	1.059	8.49	0.260	0.690	0,999	126.0	7.41	4.97
500	1.080	8.59	0.260	0.710	1.034	130.0	7.57	4.52
700	1.234	8.73	0.259	0.660	1.082	133.0	8.00	5.70
1000	1.235	8.88	0.259	0.702	1.133	135.0	8.50	4.70

It is seen in Table 1 and Fig. 7, the values of N_D, Φ_B, W_D, and E_m are a strong function of frequency and increase with increasing frequency as linearly because surface states cannot enough follow the external alternating signal at higher-frequencies. These values changed from 6.79x$0^{14}$$cm^{-3}$, 0.443 eV, 72 μm, and 1.98 kV/cm for 10 kHz to 8.88x$0^{14}$$cm^{-3}$, 1.133 eV, 135 μm, and 8.50 kV/cm for 1 M Hz, respectively. In addition, the value of N_{ss} decreases from 8.49x$0^{11}$$eV^{-1}cm^{-2}$ (at 10 kHz) to 4.70x$0^{11}$$eV^{-1}cm^{-2}$ (at 1 MHz). These lower values of N_{ss} were attributed to the passivation effect used (NiS-doped PVP) organic interlayer. In the other words, the higher value of N_{ss} at low frequencies is the result of their capability to follow the ac signal and dipole or surface polarization. All these results are indicated that N_{ss} can be able to keep up with the ac signal in both low and intermediate frequencies and hence yielded an excess capacitance and conductance to the real values. Therefore, the intercept point of the C^{-2}-V plot in the reverse bias decreases with decreasing frequency. As a result, both the surface states and polarization are usually more effective both in inversion and depletion regions, but R_s is effective only at the accumulation region.

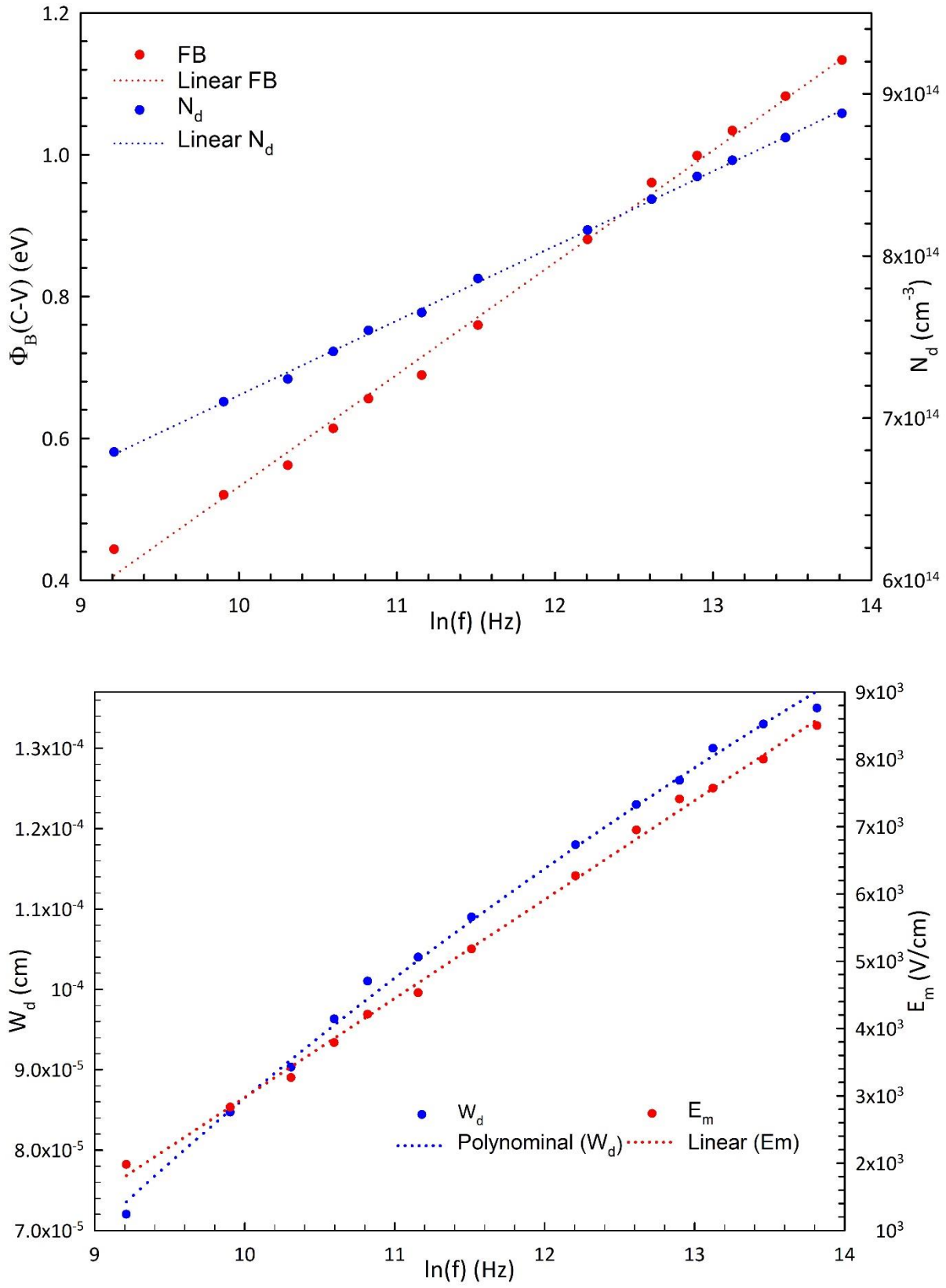

Fig. 9. **(a)** The plots of Φ_B-ln(f) and N_d-ln(f) characteristics of the Au/(NiS:PVP)/n-Si structure for various frequency and **(b)** The plots of W_d-ln(f) and (b) E_m-ln(f) characteristics of the Au/(NiS:PVP)/n-Si structure for various frequency.

The voltage or energy-dependent profile of N_{ss} can be determined by several methods such as Hill-Coleman, low-high capacitance (C_{lf}-C_{hf}), and admittance or parallel- conductance [8, 14-16]. Among them, the first method (Hill-Coleman) is valid only when C-V or G-V plot has a peak. The second method (C_{lf}-C_{hf}) requires only two C-V curves at enough low and intermediate-high frequency, and the last one (admittance) is a more sensitive and accurate method but requires a lot of C-V and G/w-V curves in a wide range of frequency and developed by Nicollian-Brews [4]. Therefore, voltage-dependent profiles of N_{ss} and their life-time (τ) extracted from both the low-high (10 kHz-1 MHz) and parallel-conductance techniques. Fig. 8 shows the C-V plots for10 kHz and 1 MHz and the obtained N_{ss}-V plot by using the following relation from these two plots was also represented inset in this figure.

$$qAN_{ss} = \left[(1/C_{lf} - 1(C_i)^{-1} - (1/C_{hf} - 1/C_i)^{-1}\right] \tag{9}$$

In Eq.9, C_i is the interfacial layer capacitance that can be obtained by using the value of C and G at adequate high frequency at the accumulation region as follow [4]. As can be seen inset in Fig. 8, the N_{ss}-V plot has peak behavior due to a special density-distribution of N_{ss} between polymer layer and semiconductor in forbidden-bandgap of Si. It is clear that the observed discrepancies in low (10 kHz) and high frequency (1 MHz) C-V plots both in inversion and depletion are the result of existence N_{ss} and polarization at low frequency, but is the result of Rs at high frequency at accumulation layer. Therefore, it is more important to take of N_{ss} and R_s effects in the C-V and G-V characteristics.

$$C_i = C_{ma}(1 + (G_{ma}/\omega C_{ma})^2) \tag{10}$$

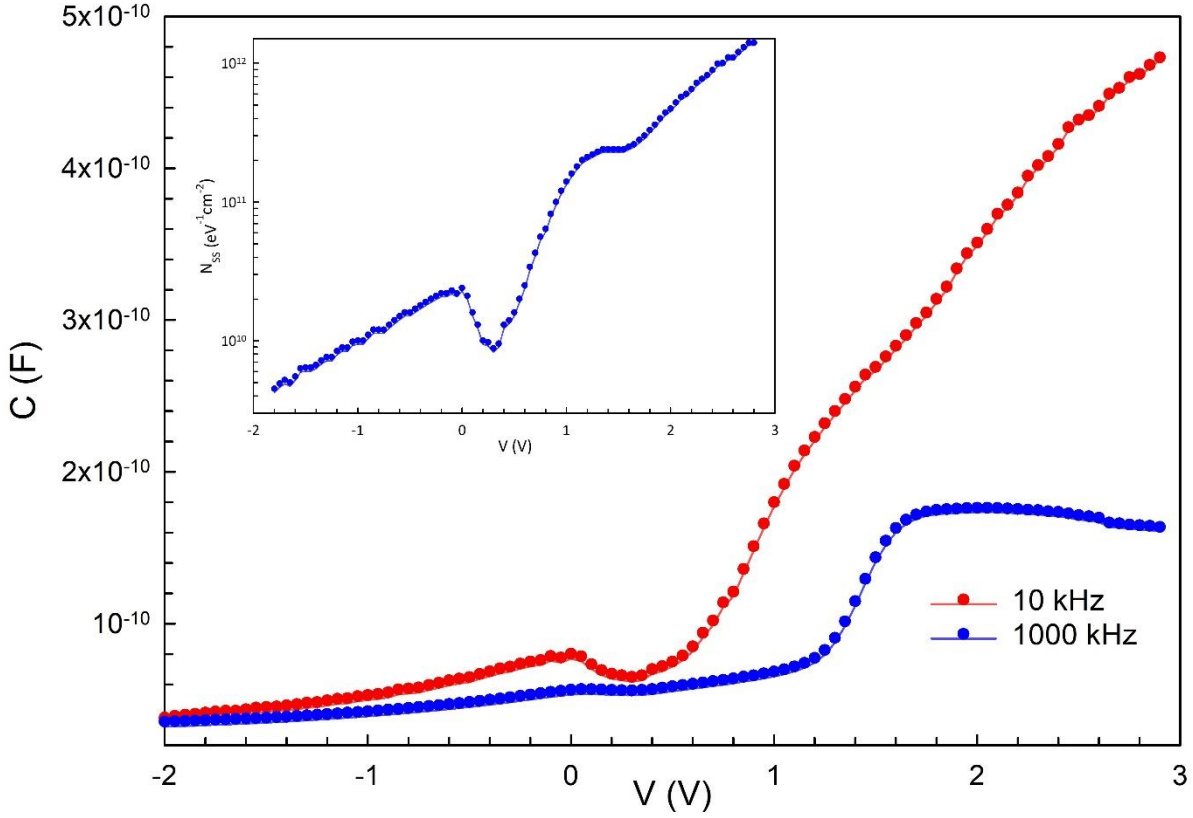

Fig. 10. The plots of (C_{lf}-C_{hf}) curves and inset Nss-V curve of the Au/(NiS:PVP)/n-Si structure.

For more elucidation of the voltage and frequency effects on the C and G/ω values, both the semi-logarithmic C- f and G/ω-f plots were also drawn and given in Figs. 9 and 10 between 0.4 V and 2 V by 50 mV steps, respectively. It is observed, both the C and G/ω values decrease with an increasing frequency almost as exponentially. According to Nicollian and Goetzberger, the parallel conductance values (G_p/ω) can be also extracted from Fig. 9. and 10 as given Eq. 6 [4].

$$\frac{G_p}{\omega} = \frac{\omega C_i^2 (G_m - \omega^2 C_m^2 R_s - R_s G_m^2)}{(\omega^2 C_{ox} R_s C_m - G_m)^2 + \omega^2 (Ci - C_m - C_{ox} R_s G_m)^2}$$
$$\cong (\omega C_m C_i^2)/((G_m^2 + \omega^2 (C_i - C_m)^2) = \frac{qAN_{ss}}{2\omega\tau} \ln(1 + \omega^2 \tau_p^2) \quad (11)$$

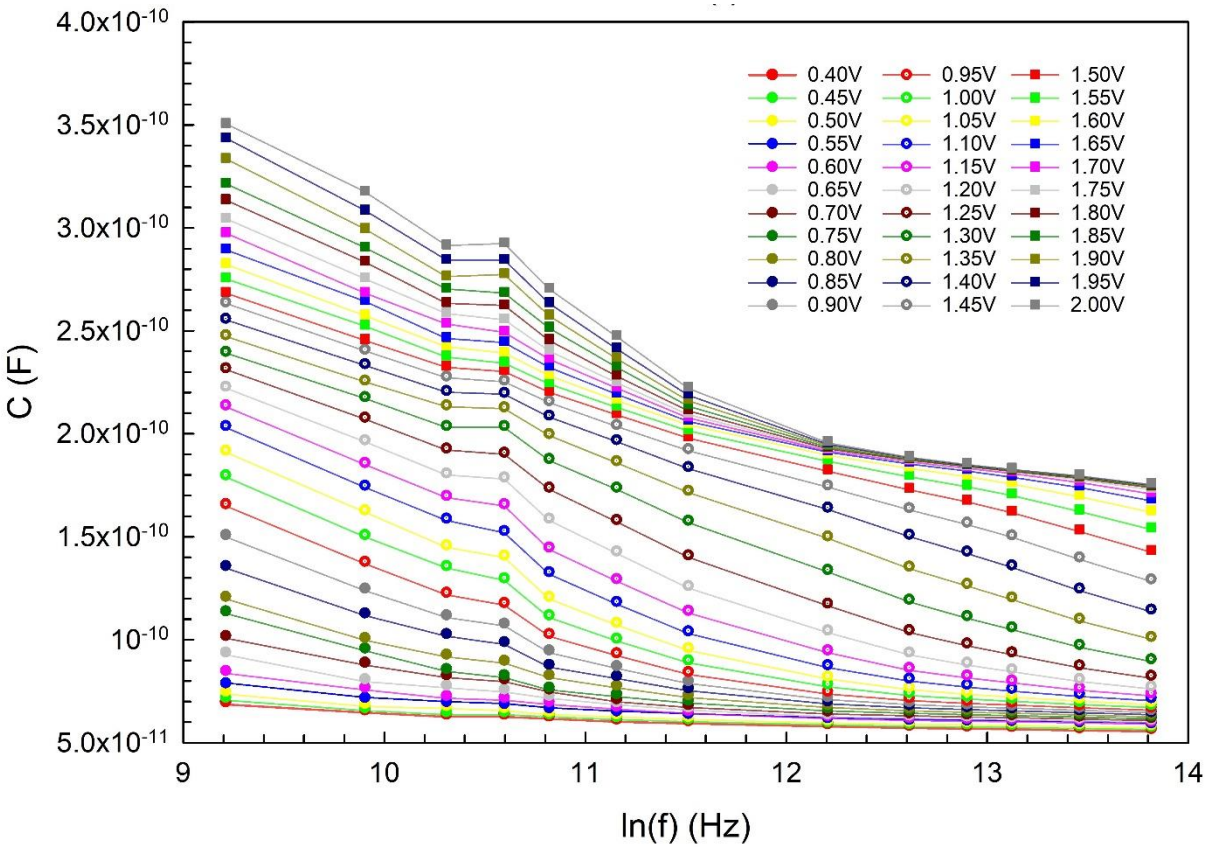

Fig. 11. The plot of C-ln(f) characteristics of the Au/(NiS:PVP)/n-Si structure for various applied bias voltages.

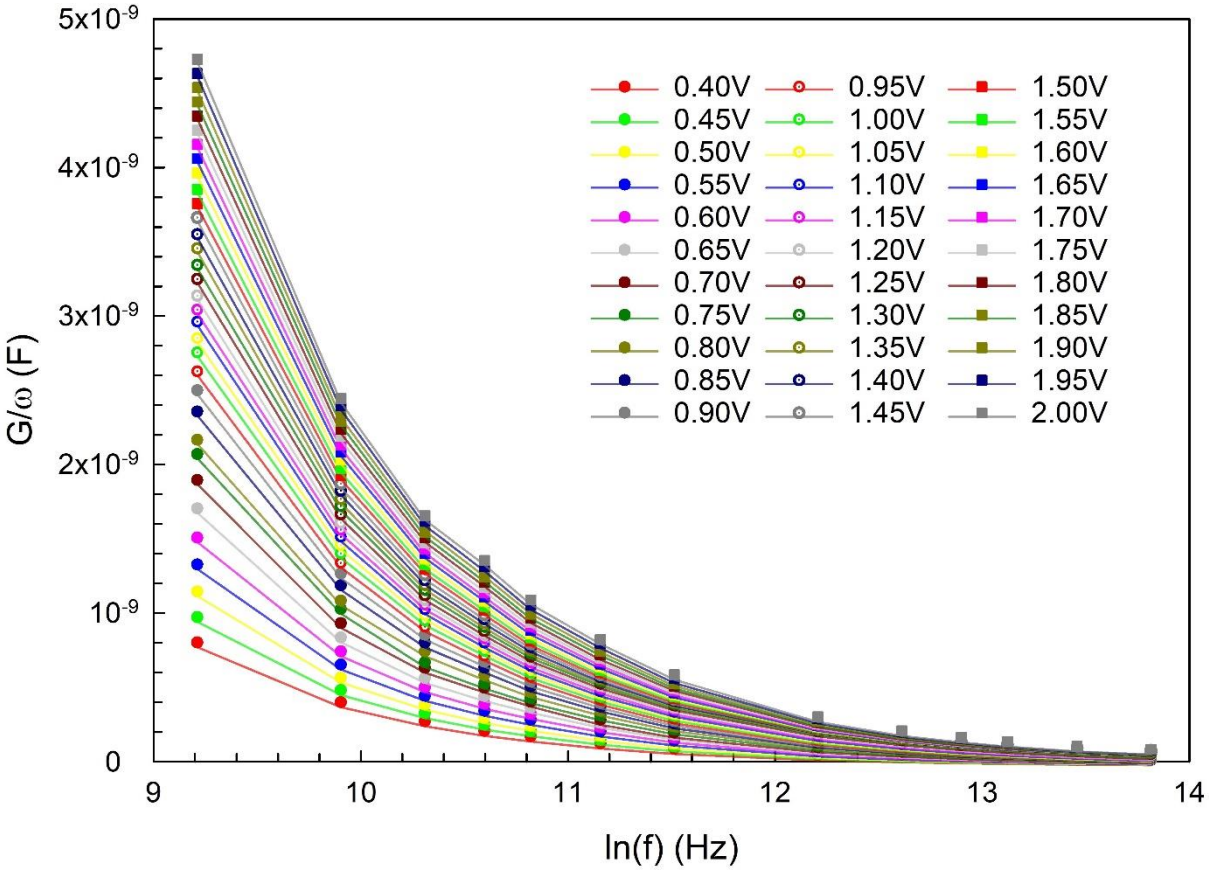

Fig. 12. The plot of G/ω-ln(f) characteristics of the Au/(NiS:PVP)/n-Si structure for various applied bias voltages.

The G_p/ω is the result of loss mechanisms occurring when surface-states/traps capture or emit charge carriers and the values of G_p/ω-ln(f) curves give a peak at $\omega=1.98/\tau$ and hence the values of N_{ss} for each bias-voltage can be obtained calculated from the peak value of these plots as follow:

$$qAN_{ss}=(G_p/\omega)_{max}/0.402 \quad (12)$$

Figure 11 shows the Gp/ω-ln(f) curves of the Au/(0.01Ni-PVA)/n-Si (MPS) structure for various forward bias voltages (0.4-2.0 V by 50 mV steps). The Gp/ω In(f) curves have a clear peak, while its magnitude increase with increasing forward bias voltage, its position shifts towards the accumulation region depend on the density of N_{ss} and their relaxation-time under external an electric field and oscillation voltage [1,4]. Such peak behavior of parallel-conductance peak was attributed restructure and reordering of charges at interface traps os states

under an external electric field. For the peak value of G_p/ω-ln(f) plot, $\omega\tau$ is equal to 1.98 and so $N_{ss}=(G_p/\omega)_{max}/(0.402qA)$. In this way, both the value of N_{ss} τ was calculated from these equations for various applied bias voltage and given in Fig. 12 and Table 2.

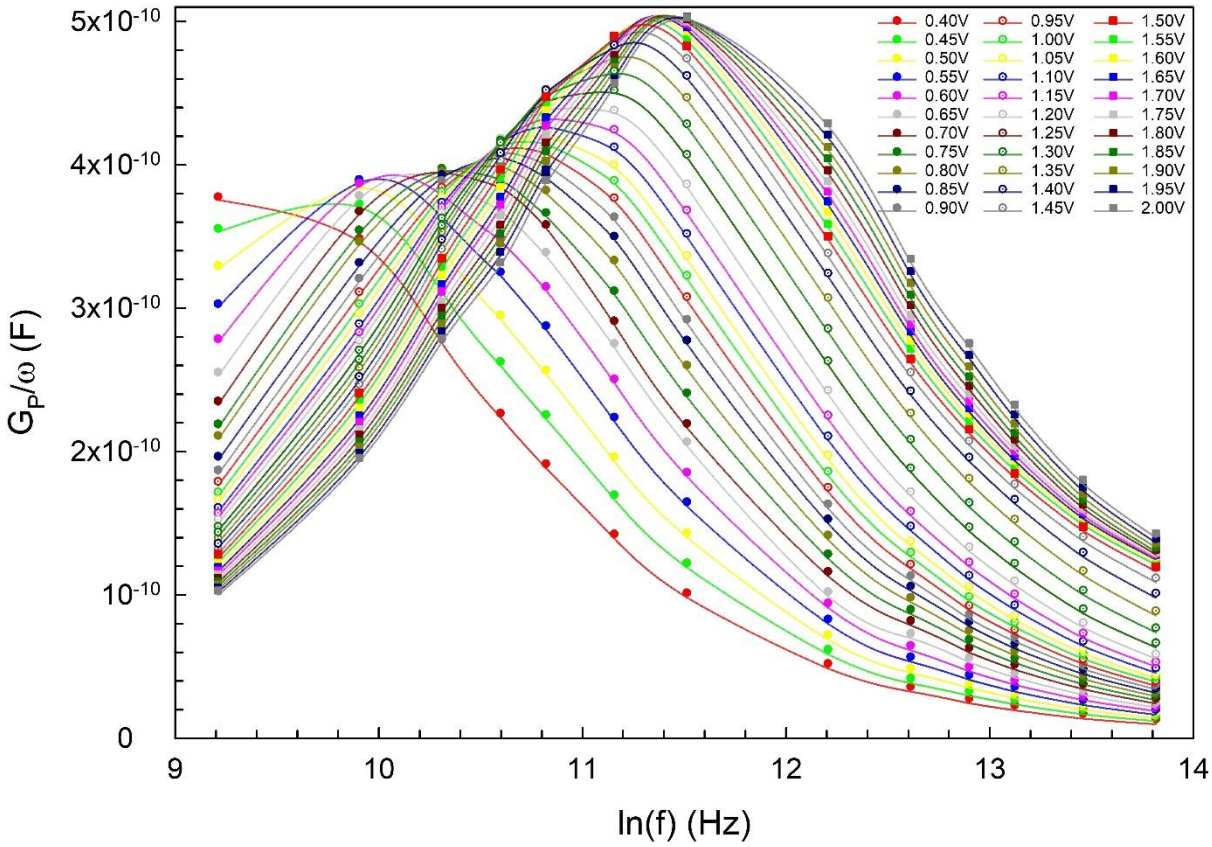

Fig. 13. The plot of G_p/ω-ln(f) characteristics of the Au/(0.01Ni-PVA)/n-Si (MPS) structure for various forward bias voltages (0.4-2.0 V by 50 mV steps).

Table 2. The values of $(G_p/\omega)_{max}$, Nss and their relaxation time (τ) of the Au/(NiS:PVP)/n-Si the structure obtained from the admittance method for various applied bias voltage.

V (V)	$(G_p/\omega)_{max}$ 10^{-10}x(F)	f 10^3x(Hz)	τ (s)	N_{ss} 10^{12}x($eV^{-1}.cm^{-2}$)
0.30	5.662	1.69	$1.87x10^{-4}$	1.121
0.35	5.736	2.45	$1.29x10^{-4}$	1.136
0.40	5.801	3.30	$9.55x10^{-5}$	1.148
0.45	5.871	4.34	$7.27x10^{-5}$	1.162
0.50	5.922	5.45	$5.79x10^{-5}$	1.172
0.55	5.947	6.51	$4.84x10^{-5}$	1.177

0.60	5.960	7.44	$4.24x10^{-5}$	1.180
0.65	5.980	8.28	$3.81x10^{-5}$	1.184
0.70	5.988	9.07	$3.48x10^{-5}$	1.185
0.75	5.996	9.75	$3.24x10^{-5}$	1.187
0.80	6.005	1.04	$3.04x10^{-5}$	1.189
0.85	6.019	1.10	$2.87x10^{-5}$	1.192
0.90	6.035	1.16	$2.73x10^{-5}$	1.195
0.95	6.055	1.21	$2.61x10^{-5}$	1.199
1.00	6.072	1.26	$2.50x10^{-5}$	1.202
1.05	6.092	1.31	$2.41x10^{-5}$	1.206
1.10	6.102	1.36	$2.33x10^{-5}$	1.208
1.15	6.114	1.40	$2.26x10^{-5}$	1.210
1.20	6.124	1.44	$2.19x10^{-5}$	1.212
1.25	6.136	1.48	$2.13x10^{-5}$	1.215
1.30	6.134	1.51	$2.08x10^{-5}$	1.214

It is clear from both Table 2 and Fig. 12, while N_{ss} increases with increasing bias voltage, t decreases almost as exponentially. Also in Table 2, the values of N_{ss} and τ were found as $1.121x10^{12}$ $eV^{-1}cm^{-2}$ and 187 μs for 0.3 V and $1.214x10^{12}$ $eV^{-1}cm^{-2}$ and 151 μs for 1.3 V, respectively. The values of N_{ss} are in order of ~10^{12} $eV^{-1}cm^{-2}$ and this order is very suitable for such MPS and MIS type structures. These low-values of N_{ss} are the result of the passivation effect of the used (NiS-doped PVP) organic interlayer. All obtained results confirm that the utilized (NiS-doped PVP) organic interface layer can be effectively utilized instead of widely used conventional interface layers. There are also similar expressions in the different previously published literature [29-31].

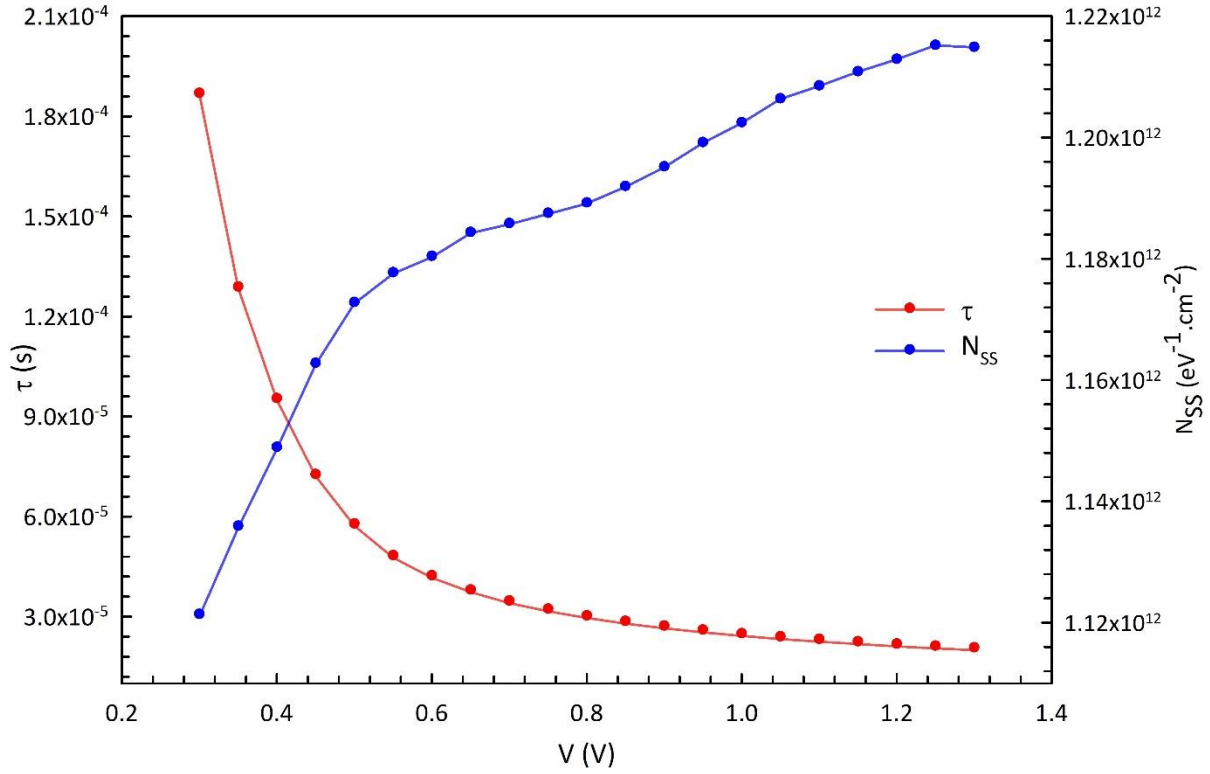

Fig. 14. The plot of N_{ss}-V and τ-V characteristics of the Au/(NiS-PVA)/n-Si (MPS) structure for various forward bias voltages (0.4-2.0 V by 50 mV steps).

4. Conclusion

Au/(NiS-PVA)/n-Si (MPS) structures were performed and then the electrophysical characteristics of them have been studied in detail. C and G/ω values were found the strong frequency dependence and electric field (E=V/d). The observed higher values of them at very low frequencies were due to the existence N_{ss} located at Au/(%1Ni-PVA) interface and polarization processes. Some main electrophysical features such as V_D, N_D, E_F, Φ_B, W_D, and E_m were calculated from the intercept and slope of reverse-bias C^{-2}-V plot for each frequency. The value of Φ_B was found to increase with increasing frequency as $\Phi_B(lnf)=(0.158x+1.055)$ eV. The values of N_D, W_D, and E_m were also found to increase with an increasing frequency almost linearly. Voltage-dependent profiles of R_s, N_{ss}, and τ were extracted from the admittance method, respectively. As can be seen in Table 2, the values of N_{ss} and τ were found as $1.121x10^{12}$ $eV^{-1}cm^{-2}$ and 187 μs for 0.3 V and $1.214x10^{12}$ $eV^{-1}cm^{-2}$ and 151 μs for 1.3 V, respectively. These values of N_{ss} are convenient for such MPS and MIS type structures is the result of the passivation effect of the used (NiS-doped PVP)

organic interlayer. NiS-doped PVP organic interlayer has some advantages in comparison with other conventional interfacial layers.

Acknowledgments

This study was supported by Gazi University Scientific Research Project. (Project Number: GU-BAP.05/2019-26)

References

1. Sze S. M. and Kwok K. Ng , Physics of Semiconductor Devices 3rd edn. (New Jersey: John Wiley & Sons), 2007
2. B. L. Sharma, Metal-semiconductor Schottky Barrier Junctions and Their Applications, Plenum Press New York, 1984.
3. E. H. Rhoderick, R. H. Williams Metal-Semiconductor Contacts (Oxford: Clarendon Press) (2nd ed), 1988.
4. E. H. Nicollian and J. R. Brews, MOS (Metal Oxide Semiconductor) Physics and Technology. New York, NY, USA: Wiley, 1982
5. E. H. Nicollian and A. Goetzberger, "The Si-SiO_2 interface Electrical properties as determined by the metal-insulator-silicon conductance technique," Bell Syst. Tech. J., 46 (1967) 1055-1133.
6. H. C. Card, E. H. Rhoderick, Studies of tunnel MOS diodes I. Interface effects in silicon Schottky diodes, J. Phys. D Appl. Phys. 4, 1589-1601 (1971)
7. Ç. G. Türk, S. Orkun Tan, Ş. Altındal, B. İnem, Frequency and voltage dependence of barrier height, surface states, and series resistance in Al/Al_2O_3/p-Si structures in wide range frequency and voltage, Physica B, 582 (2020) 411979.
8. M. Sharma, S.K. Tripathi, Frequency and voltage dependence of admittance characteristics of Al/Al_2O_3/PVA:n-ZnSe Schottky barrier diodes. Mater. Sci. Semicond. Process. 41 (2016) 155-161.
9. S. Altindal Yeriskin, The investigation of effects of (Fe_2O_4-PVP) organic-layer, surface states, and series resistance on the electrical characteristics and the sources of them, J. Mater Sci, Mater in Electron, 30 (2019) 17032-17039.
10. A. Buyukbas-Ulaşan, S. Altındal Yerişkin, A. Tataroğlu, M. Balbaşı, Y. Azizian Kalandaragh, "Electrical and impedance properties of MPS structure based on (Cu_2O-CuO-PVA) interfacial layer, J. Mater. Sci.: Mater. In Electron., 29 (2018), 8234-8243.
11. S. Altındal Yerişkin, M. Balbaşı, İ. Orak, The effects of (graphene doped-PVA) interlayer on the determinative electrical parameters of the Au/n-Si (MS) structures at room temperature. J Mater Sci Mater Electron 28 (2017)14040-14048.
12. M.S. Paratap Reddy, J.H. Lee, J.S. Jang, Frequency-dependent series resistance and interface states in Au/bio-organic/n-GaN Schottky structures based on DNA biopolymer, Synth. Met., 185 (2013) 167-171.
13. B. Akın, Ş. Altındal, On the frequency and voltage-dependent main electrical parameters of the Au/ZnO/n-GaAs structures at room temperature by using various methods, Physica B: Physics of Condensed Matter, 594 (2020) 412274.
14. G. Ersöz, İ. Yücedağ, Y. Azizian-Kalandaragh, İ. Orak, Ş. Altındal, Investigation of electrical characteristics in Al/CdS-PVA/p-Si (MPS) structures using impedance spectroscopy method. IEEE Trans. Electron Devices **63** (2016) 2948-2955.

15. M.S. Pratap Reddy, K. Sreenu, V. Rajagopal Reddy, C. Park, Modified electrical properties and transport mechanism of Ti/p-InP Schottky structure with a polyvinyl-pyrrolidone (PVP) polymer interlayer, J. Mater. Sci. Mater. Electron. 28 (2017) 4847-4855.
16. İ. Taşçıoğlu, M. Soylu, Ş. Altındal, A.A. Al-Ghamdi, F. Yakuphanoğlu, Effects of interface states and series resistance on electrical properties of Al/nanostructure CdO/p-GaAs diode, J. Alloy. Compd., 541 (2012) 462-467.
17. Ç. Bilkan, Ş. Altındal, Y. Azizian-Kalandaragh, Investigation of frequency and voltage dependence surface states and series resistance profiles using admittance measurements in Al/p-Si with Co_3O_4-PVA interlayer structures, Phys. B Condens. Matter, 515 (2017) 28-33.
18. L.Wanga, L. Zhanga, and M. Tian, "Improved polyvinylpyrrolidone (PVP)/graphite nanocomposites by solution compounding and spray drying", Polymers Advanced Technologies, 23 (2012) 652-659.
19. A. Tataroğlu, Ş. Altındal, Y. Azizian-Kalandaragh, "C-V-f and G/ω-V-f characteristics of Au/(In_2O_3-PVP)/n-Si (MPS) structure", Physica B: Physics of Condenced Matter, 582 (2020) 411996.
20. A. Kaya, Ö. Sevgili, Ş. Altındal, Energy density distribution profiles of surface states, relaxation time and capture cross-section in Au/n-type 4H-SiC SBDs by using admittance spectroscopy method, Int J Mod Phys B, 28 (2014) 1450104.
21. S. Alptekin, S. O. Tan, Ş. Altındal, "Determination of Surface States Energy Density Distributions and Relaxation Times for a Metal-Polymer-Semiconductor Structure" IEEE Trans. on Nanotechnology, 18 (2019), 1196-1199.
22. İ. Dökme, T. Tunç, İ. Uslu,Ş. Altındal, The Au/polyvinyl alcohol (Co, Zn-doped)/n-type silicon Schottky barrier devices. Synth Met 161(2011)474-480.
23. Ç. Bilkan, Y. Azizian-Kalandaragh, Ö. Sevgili, Ş. Altındal, Investigation of the efficiencies of the (SnO2-PVA) interlayer in Au/n-Si (MS) SDs on electrical characteristics at room temperature by comparison, Journal of Materials Science: Materials in Electronics. 30 (2019) 20479-20488.
24. V.R. Reddy, Electrical properties of Au/polyvinylidene fluoride/n-InP Schottky diode with polymer interlayer, Thin Solid Films. 556 (2014) 300-306.
25. A. Turut, A. Karabulut, K. Ejderha, and N. Bıyıklı, "Capacitance–conductance–current–voltage characteristics of atomic layer deposited Au/Ti/Al_2O_3/n-GaAs MIS structures," Mater. Sci. Semicond. Process., 39 (2015) 400-407.
26. H. Tecimer, H. Uslu, Z.A. Alahmed, F. Yakuphanoğlu, Ş.Altındal, On the frequency and voltage dependence of admittance characteristics of Al/PTCDA/P-Si (MPS) type Schottky barrier diodes (SBDs), Composites: Part B 57 (2014) 25-30.
27. H. Tecimer, S. O. Tan, Ş. Altındal, Frequency-Dependent Admittance Analysis of the Metal-Semiconductor Structure with an Interlayer of Zn-Doped Organic Polymer Nanocomposites, IEEE Trans on Electron Dev, 65 (2018) 231-236.
28. L.L. Hench, J.L. West, Principles of electronic ceramics, Willey, New York, 1990.
29. S Zeyrek, E Acaroğlu, Ş Altındal, S Birdoğan, M.M. Bülbül, The effect of series resistance and interface states on the frequency dependent C-V and G/w-V characteristics of Al/perylene/p-Si MPS type Schottky barrier diodes, Current Applied Physics 13 (7), 1225-1230
30. G. Demir Ersöz, İ. Yücedağ, S. Altındal Yerişkin, Characterization of surface states and their relaxation time in Al/ZnO/p-GaAS structure by admittance method at room temperature, J. Mater. Sci. Mater. Electron. 14 (2019) 653-659.
31. İ Taşçıoğlu, Ö. Sevgili, Y Azizian-Kalandaragh, Ş, Altındal, Frequency-dependent admittance analysis of Au/n-Si structure with $CoSO_4$-PVP interfacial layer, Journal of Electronic Materials 49 (2020) 3720-3727.

Figures

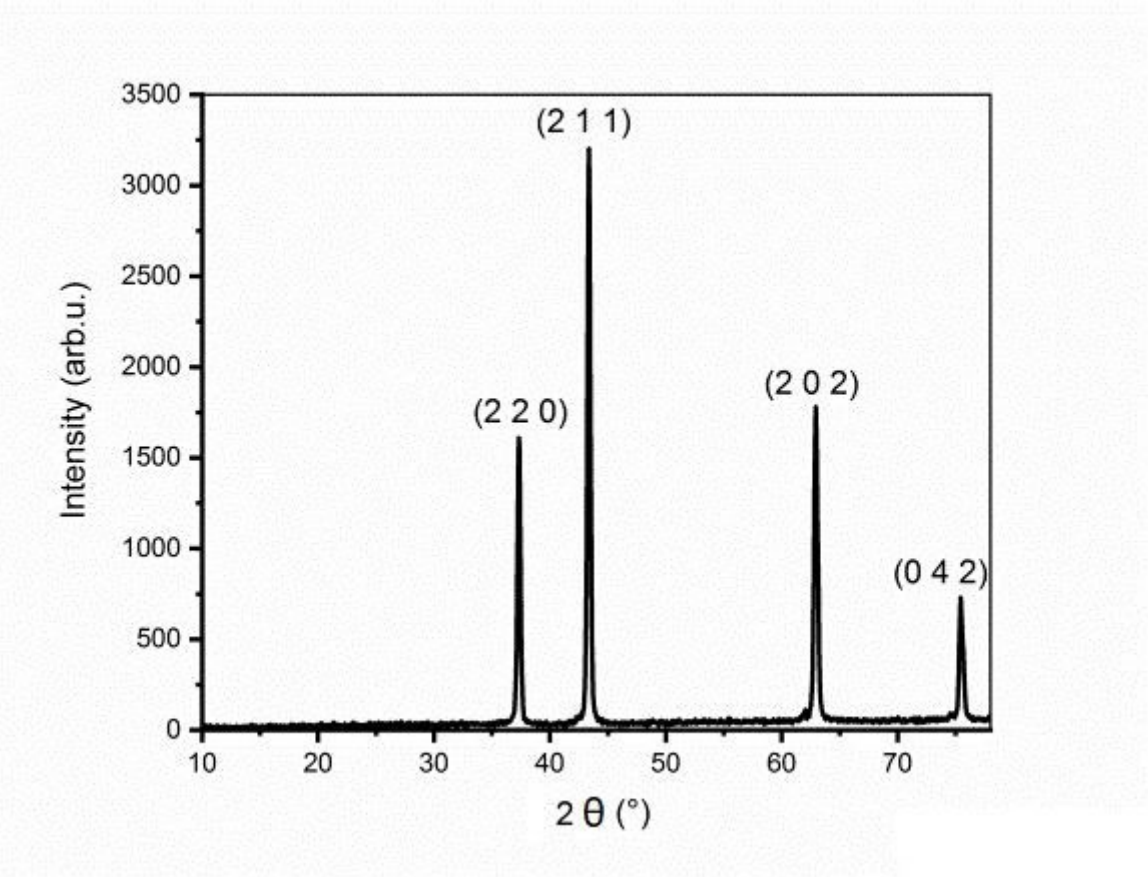

Figure 1

XRD pattern of NiS nanostructures prepared by microwave- assisted method

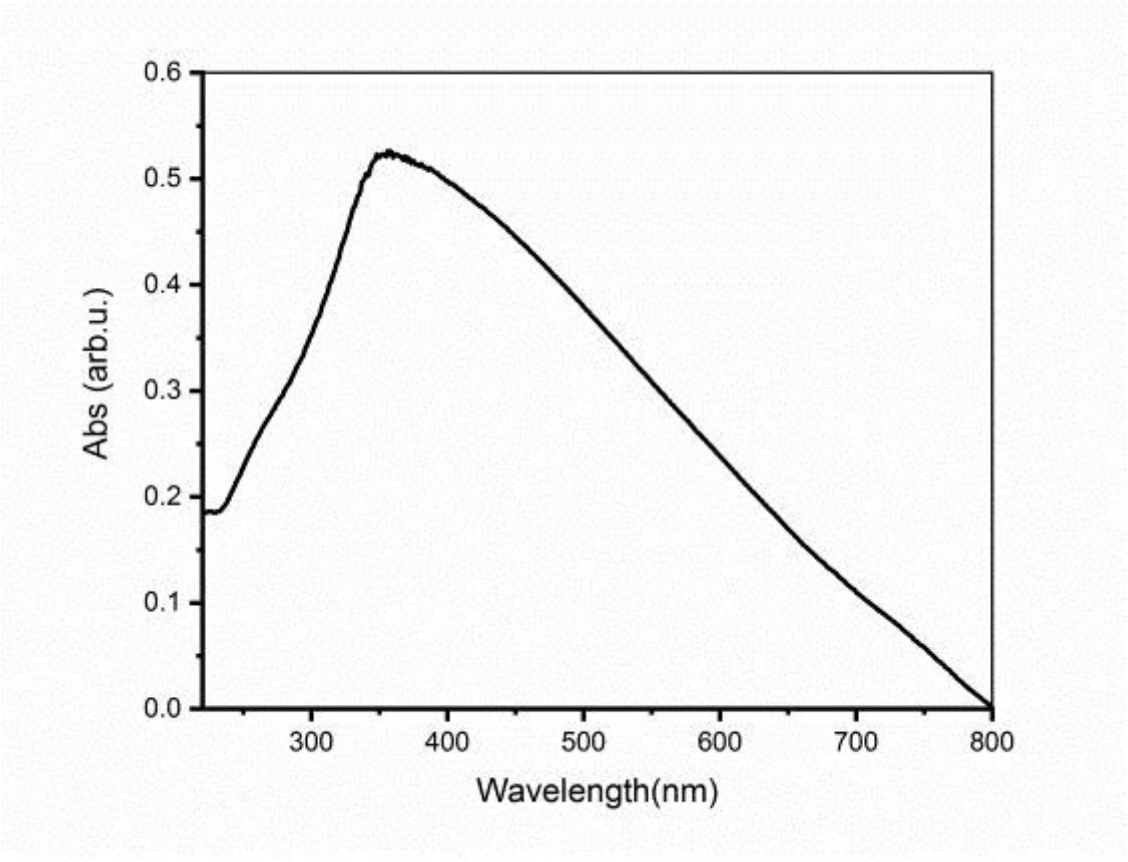

Figure 2

Absorbance spectrum of NiS nanostructures prepared by microwave- assisted method

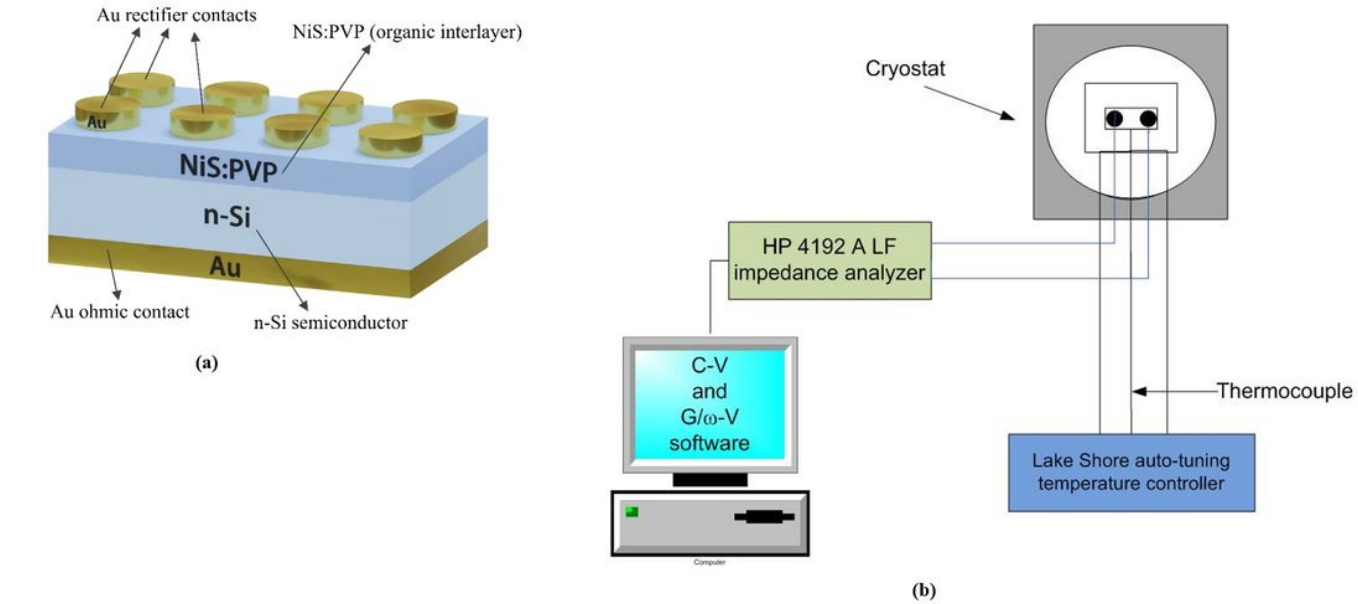

Figure 3

a) A schematic diagram of the Au/(NiS:PVP)/n-Si structures and b) the setup of the measured admittance/impedance measured system

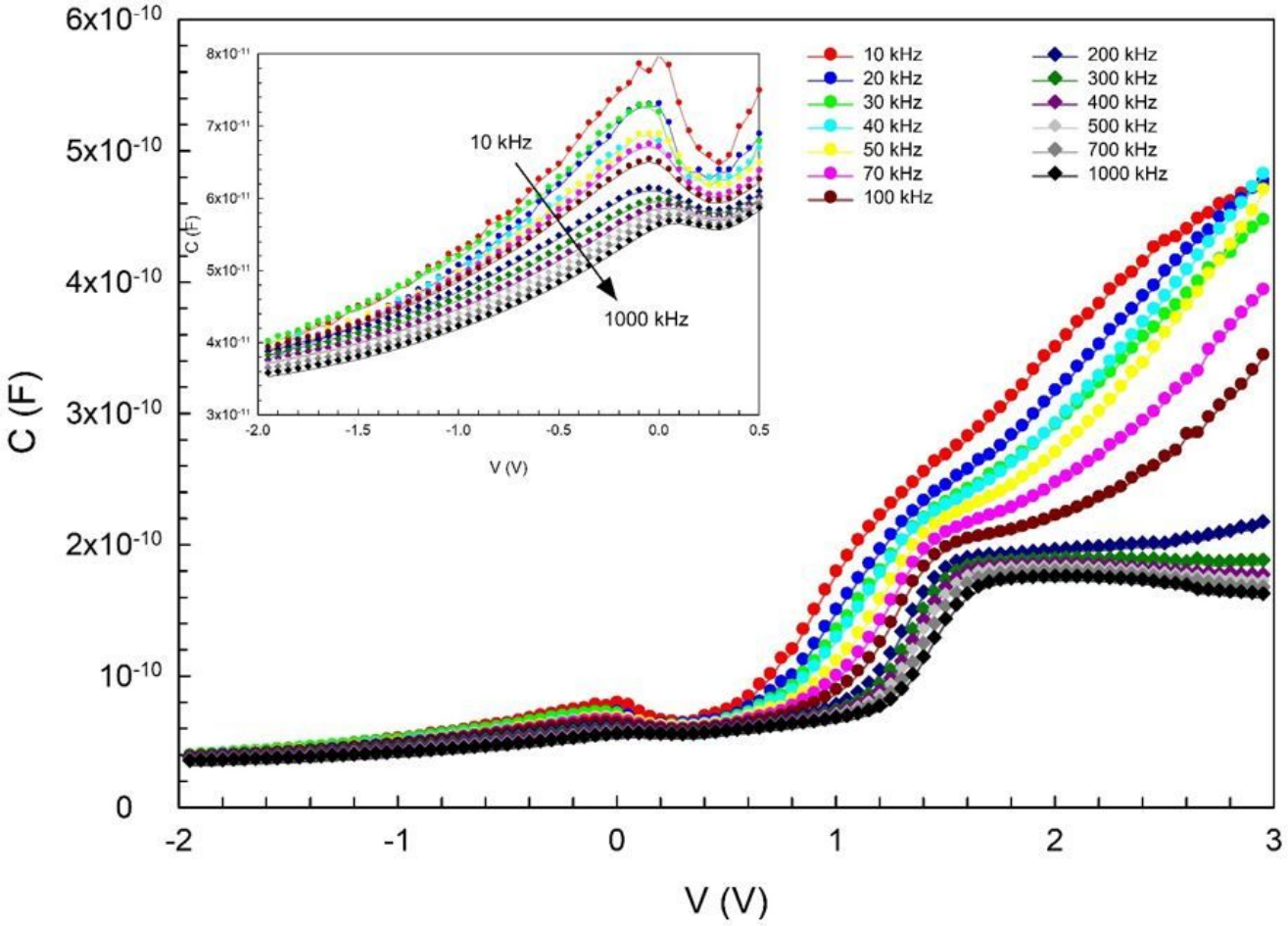

Figure 4

The plot of C-V characteristics of the Au/(NiS:PVP)/n-Si structure for various frequency.

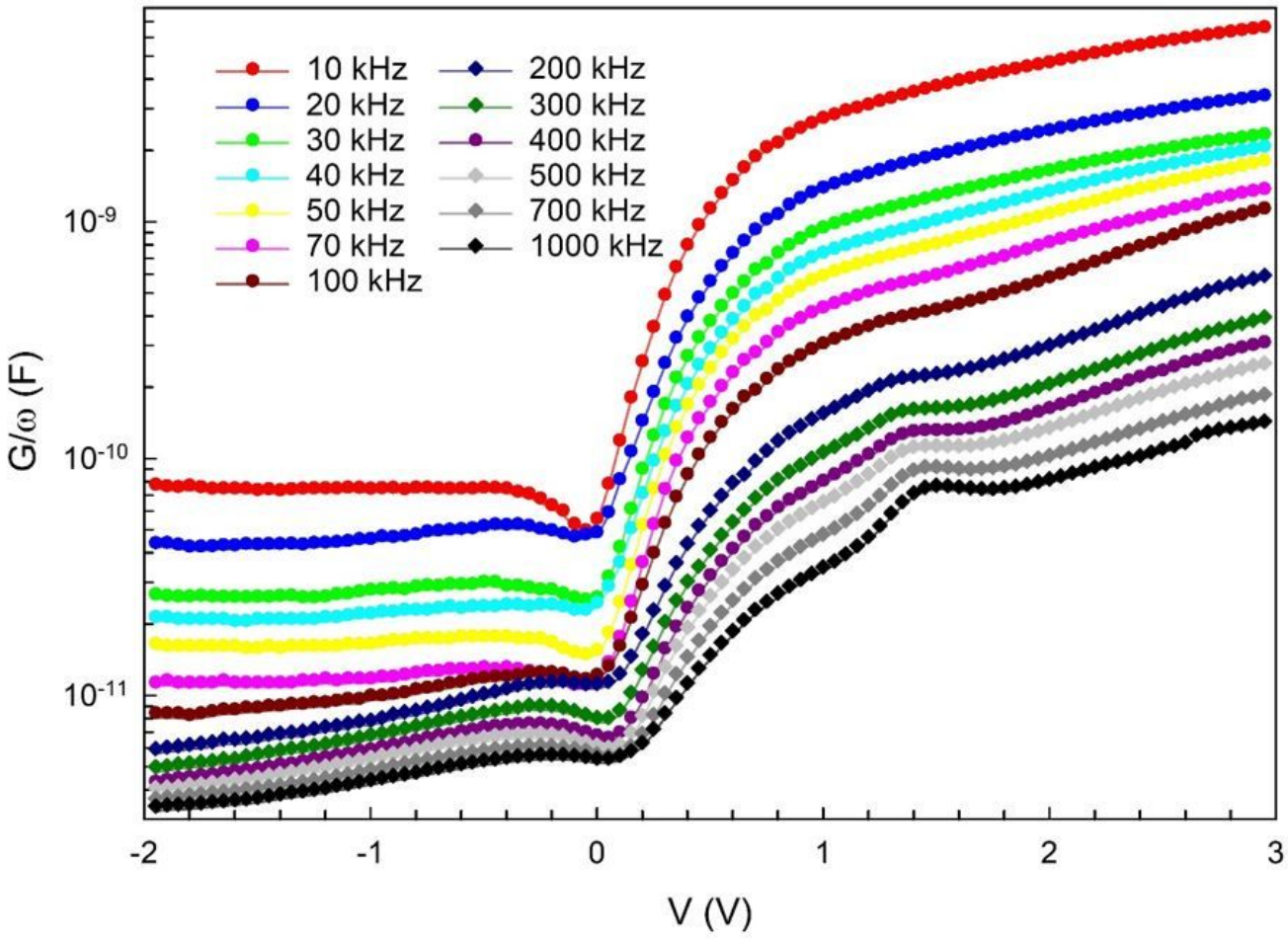

Figure 5

The plot of G/ω-V characteristics of the Au/(NiS:PVP)/n-Si structure for various frequency.

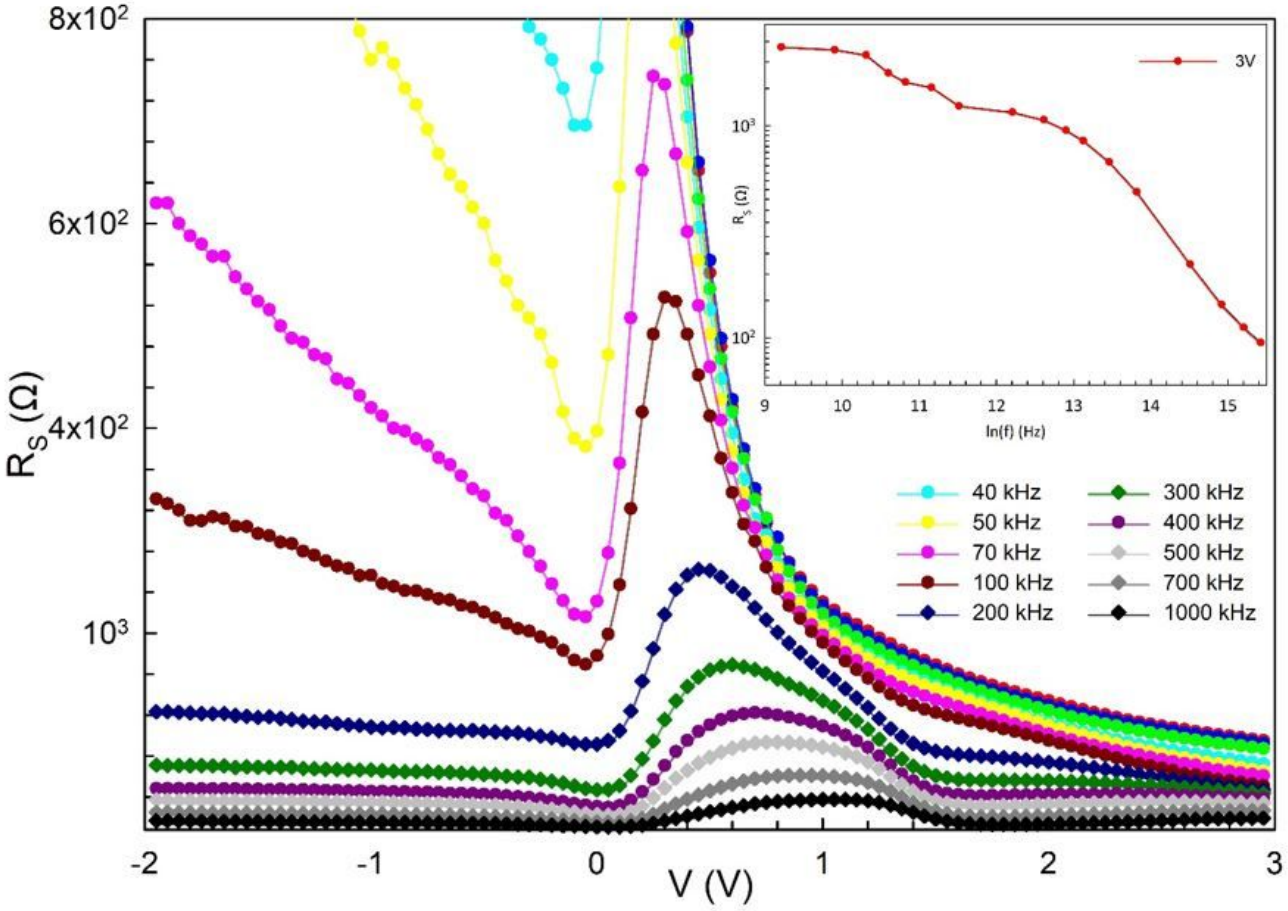

Figure 6

The plot of Ri-V and Rs-ln(f) characteristics of the Au/(NiS:PVP)/n-Si structure for various frequencies.

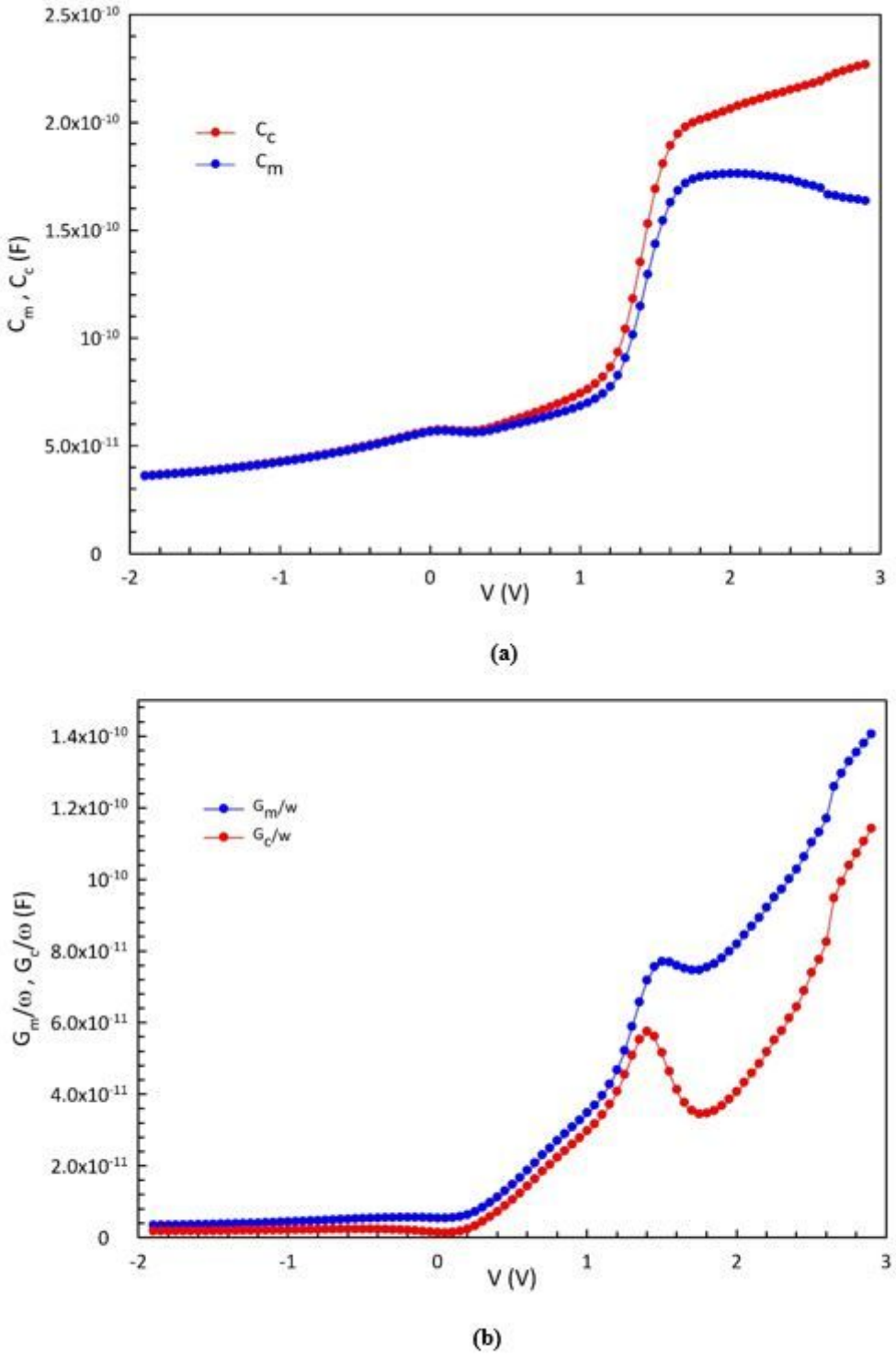

Figure 7

please see the manuscript file for the full caption

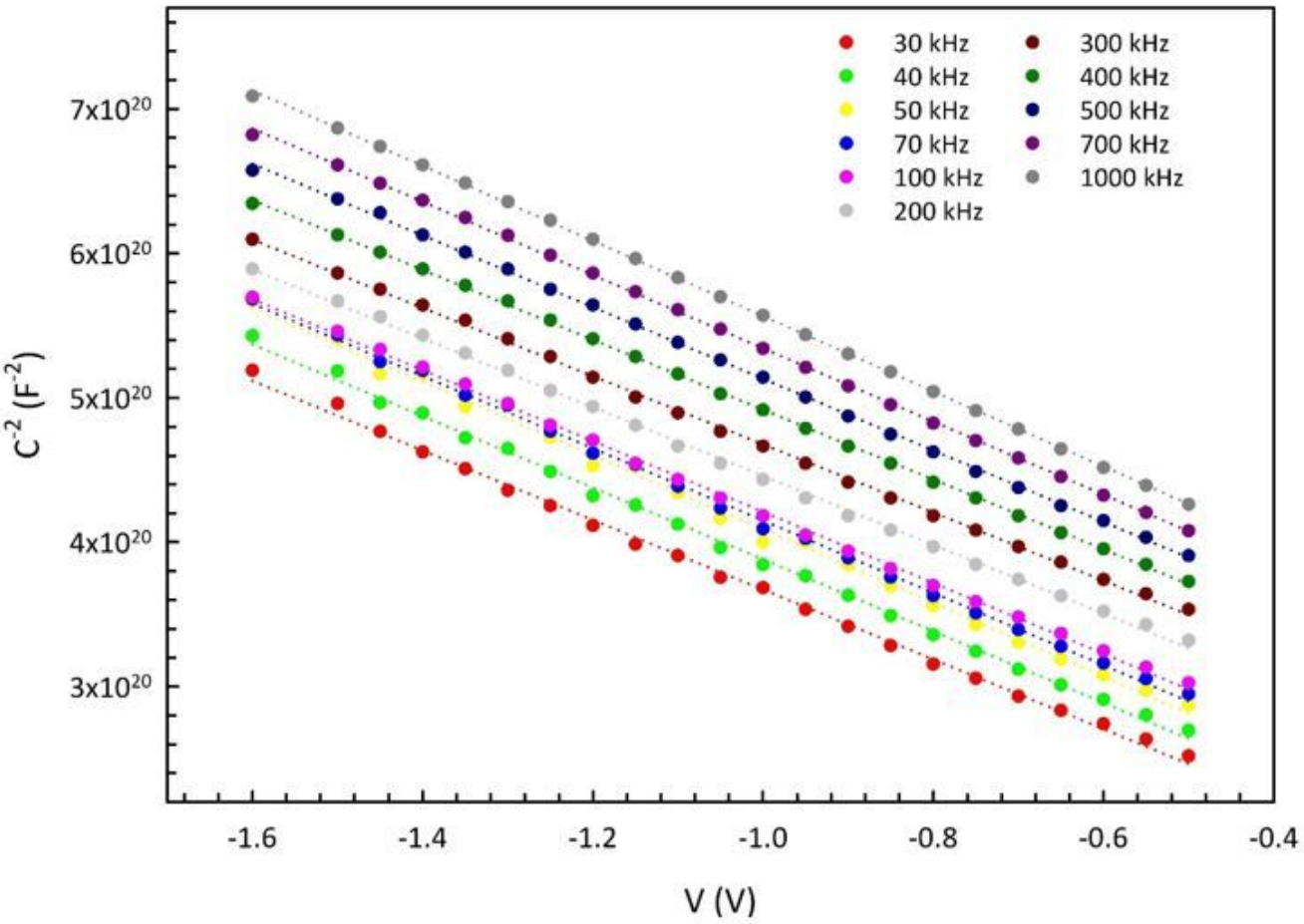

Figure 8

The plot of C-2-V characteristics of the Au/(NiS:PVP)/n-Si structure was measured for various frequencies.

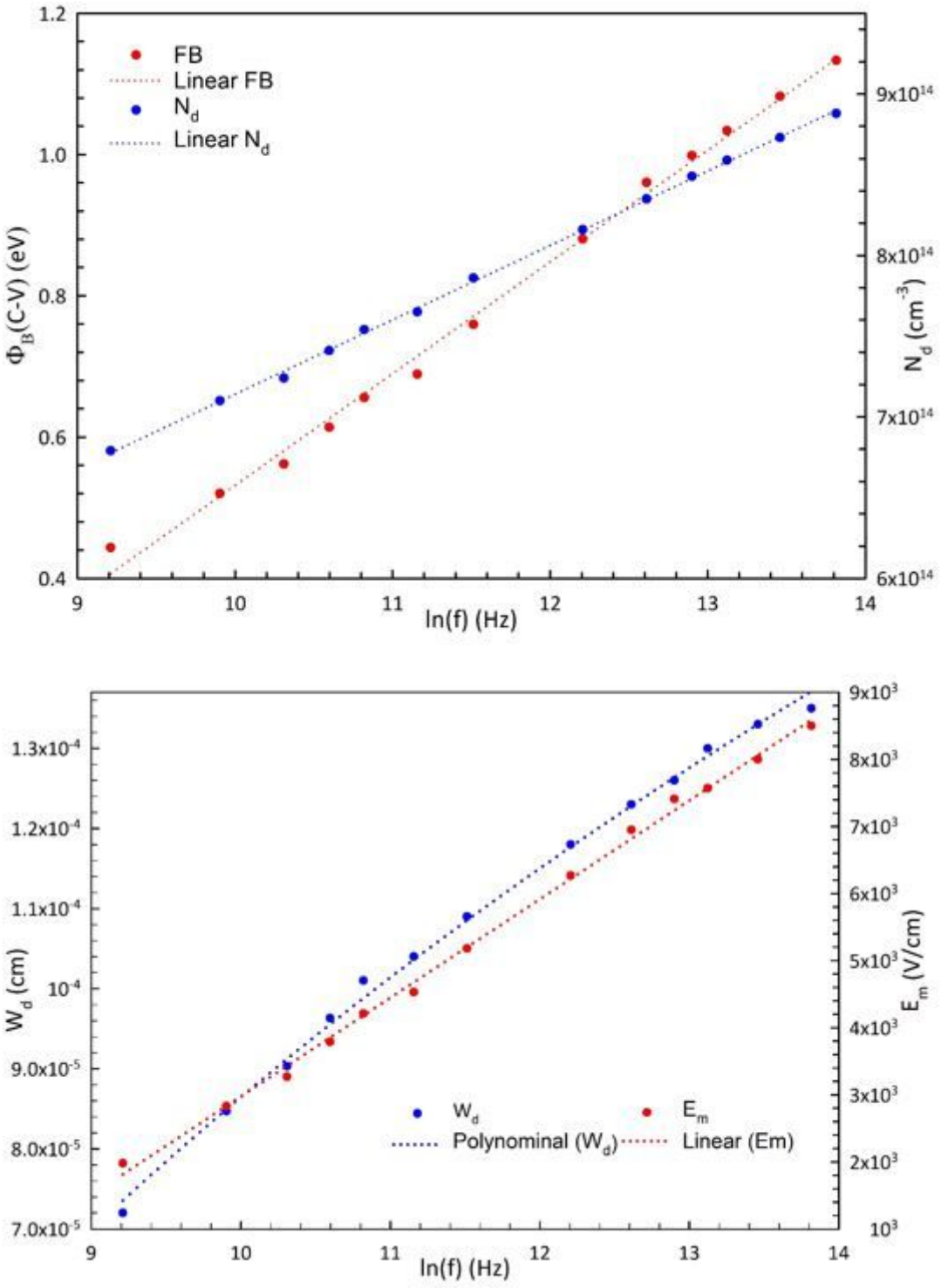

Figure 9

please see the manuscript file for the full caption

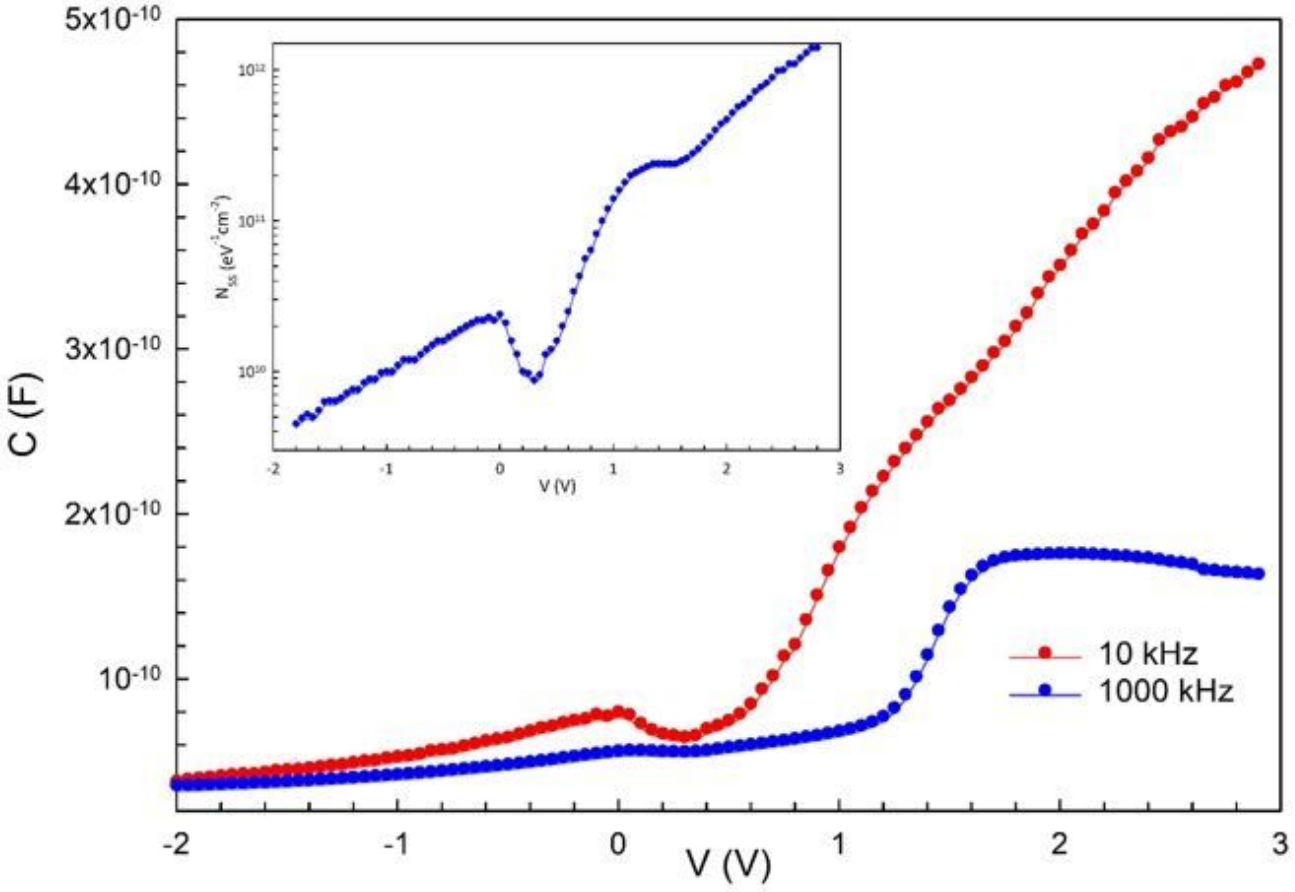

Figure 10

The plots of (Clf-Chf) curves and inset Nss-V curve of the Au/(NiS:PVP)/n-Si structure.

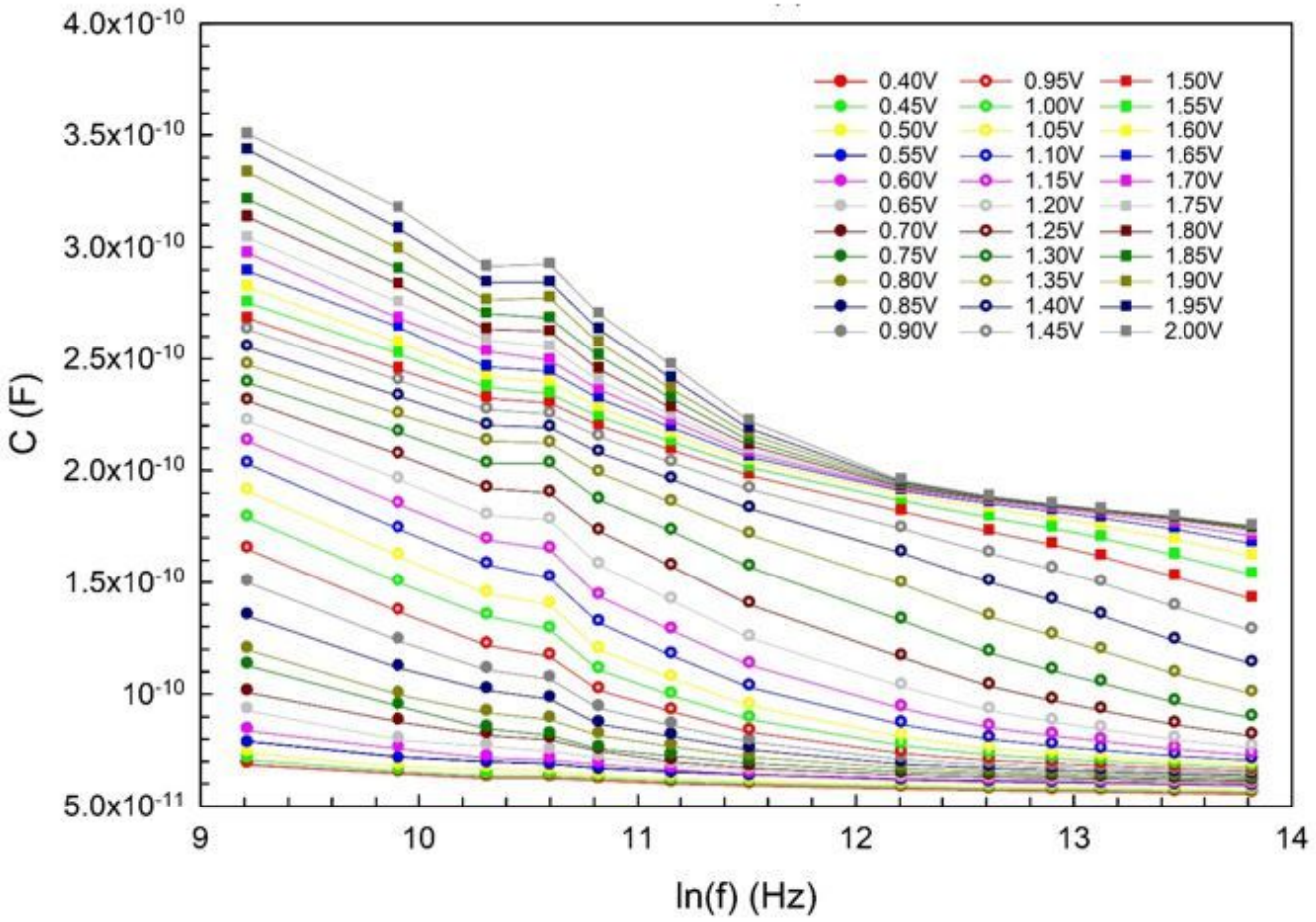

Figure 11

The plot of C-ln(f) characteristics of the Au/(NiS:PVP)/n-Si structure for various applied bias voltages.

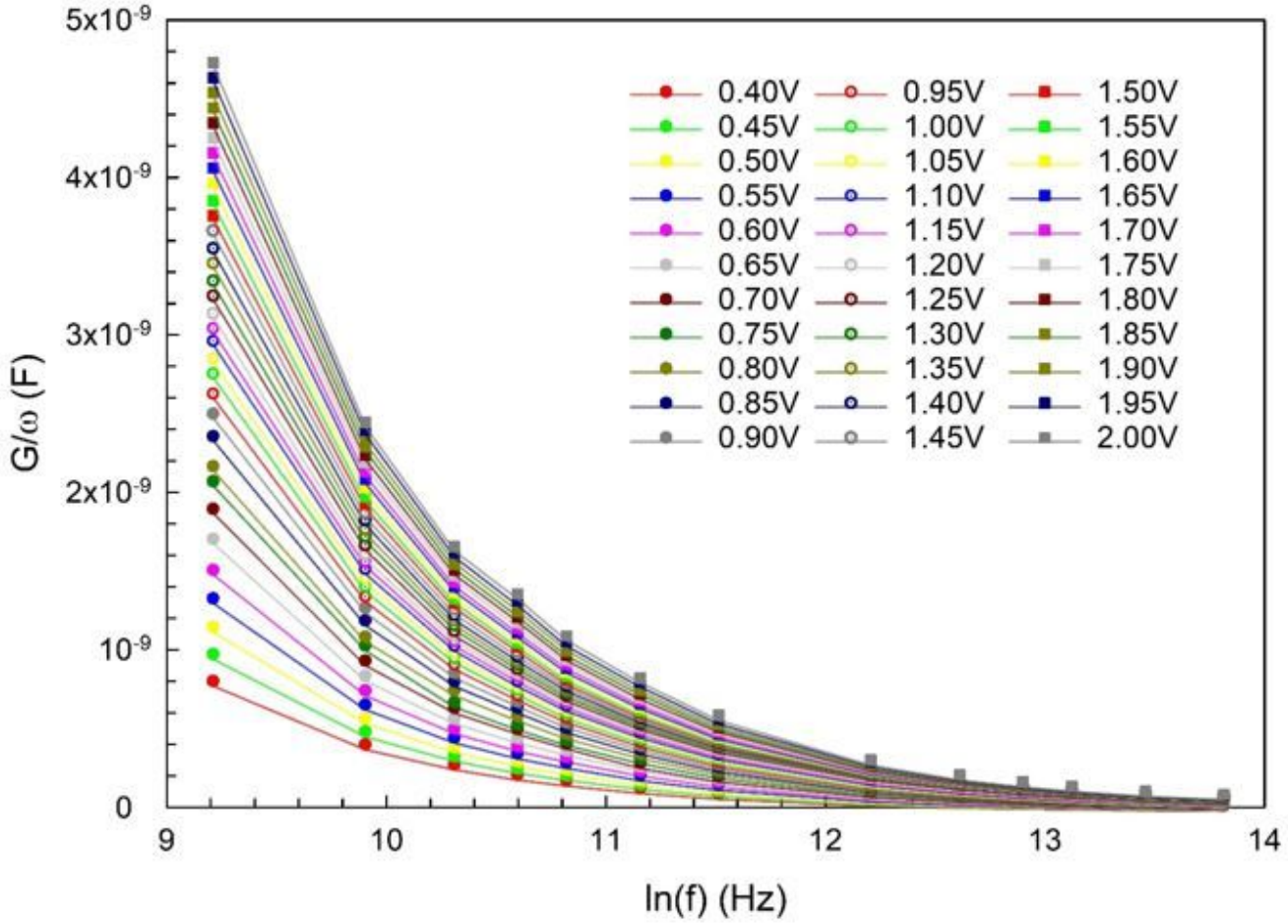

Figure 12

please see the manuscript file for the full caption

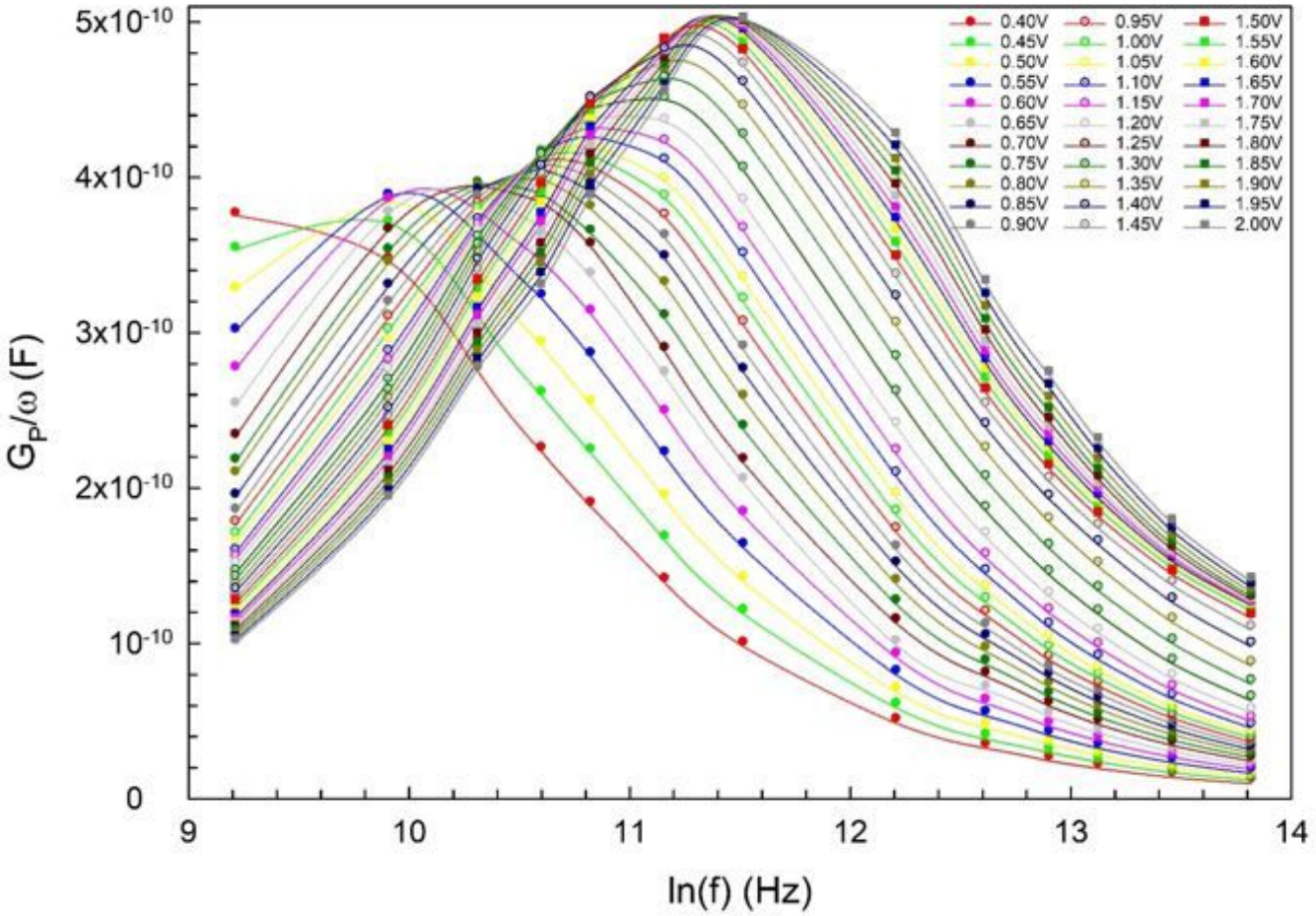

Figure 13

please see the manuscript file for the full caption

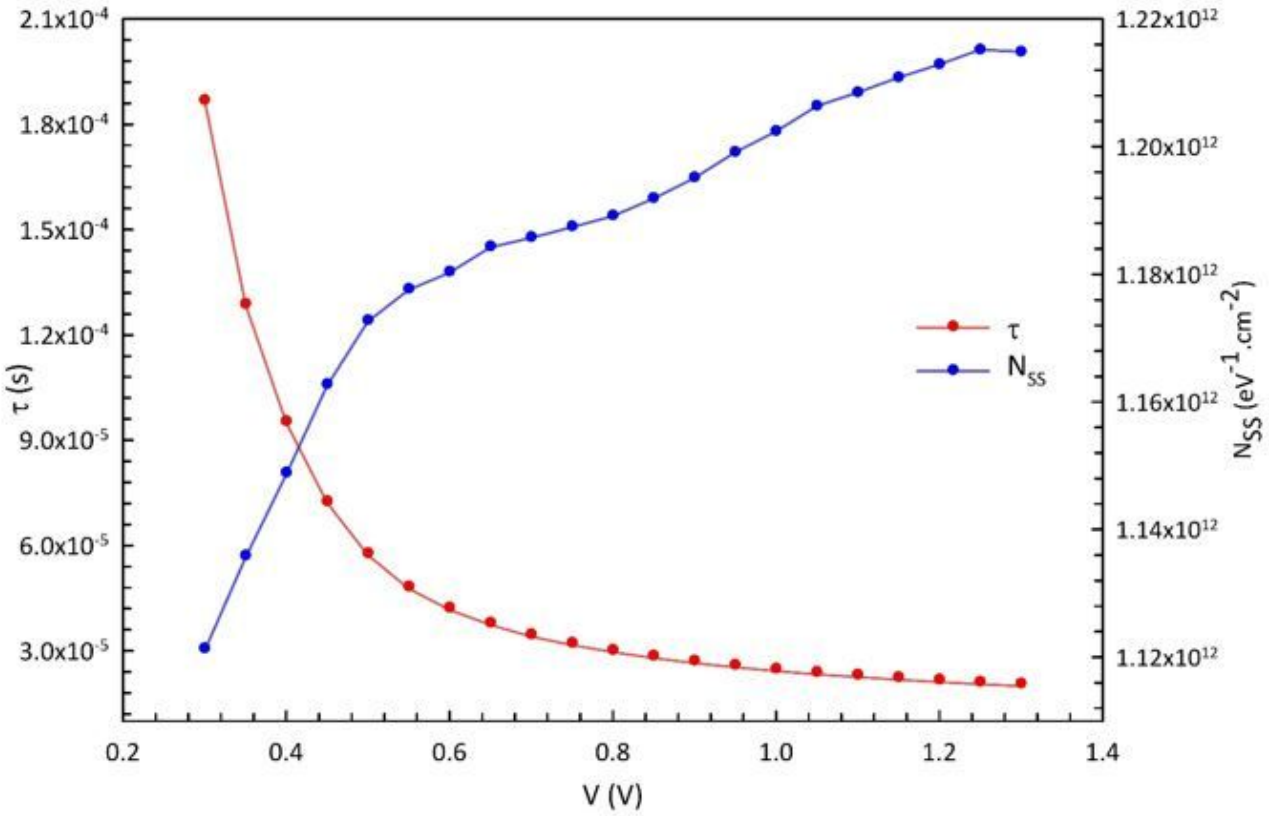

Figure 14

please see the manuscript file for the full caption